2023

U.S. Department of Transportation Federal Highway Administration

NEBRASKA DEPARTMENT OF TRANSPORTATION

NEBRASKA TRANSPORTATION CENTER

Final Report SPR-FY22(001)

Low-Cement Concrete Mixture for Bridge Decks and Rails

George Morcous, PhD, PE FPCI
Professor
Durham School of Architectural Engineering and Construction
University of Nebraska-Lincoln

Jiong Hu, PhD
Professor
Department of Civil and Environmental Engineering
University of Nebraska-Lincoln

Soumitra Das, MSc
Graduate Research Assistant
Durham School of Architectural Engineering and Construction
University of Nebraska-Lincoln

Nebraska Department of Transportation Research
Headquarters Address
1400 Nebraska Parkway
Lincoln, NE 68509
ndot.research@nebraska.gov
(402) 479-4697
https://dot.nebraska.gov/business-center/research/

Nebraska Transportation Center
262 Prem S. Paul Research Center at Whittier School
2200 Vine Street
Lincoln, NE 68583-0851
(402) 472-1932
http://ntc.unl.edu

This report was funded in part through grant from the U.S. Department of Transportation Federal Highway Administration. The views and opinions of the authors expressed herein do not necessarily state or reflect those of the U.S. Department of Transportation.

Low-Cement Concrete Mixture for Bridge Decks and Rails

George Morcous, PhD, PE, FPCI
Professor
Durham School of Architectural Engineering and Construction
University of Nebraska-Lincoln

Jiong Hu, PhD
Professor
Department of Civil and Environmental Engineering
University of Nebraska-Lincoln

Soumitra Das, MSc
Graduate Research Assistant
Durham School of Architectural Engineering and Construction
University of Nebraska-Lincoln

Sponsored By

Nebraska Department of Transportation and U.S. Department of Transportation Federal Highway Administration

December 08, 2023

TECHNICAL REPORT DOCUMENTATION PAGE

1. Report No. SPR-FY22(001)	2. Government Accession No.	3. Recipient's Catalog No.
4. Title and Subtitle Low-Cement Concrete Mixture for Bridge Decks and Rails		5. Report Date December 08, 2023
		6. Performing Organization Code
7. Author(s) Soumitra Das, George Morcous, and Jiong Hu		8. Performing Organization Report No.
9. Performing Organization Name and Address University of Nebraska-Lincoln College of Engineering Peter Kiewit Institute, 1110 S 67th St., Omaha, NE 68182-0178		10. Work Unit No. 11. Contract
12. Sponsoring Agency Name and Address Nebraska Department of Transportation 1400 Nebraska Parkway, PO Box 94759, Lincoln, NE 68509		13. Type of Report and Period Covered 14. Sponsoring Agency Code

15. Supplementary Notes

16. Abstract

Right after construction, drying shrinkage of restrained concrete bridge decks and rails causes early-age cracking, insertion of water and chemicals, and corrosion of reinforcing steel that eventually leads to delamination and spalling of concrete. The main objective of this research is to control early-age shrinkage cracking by reducing cementitious material content in bridge deck and rail concrete mixtures. Several reduced cementitious materials concrete (RCMC) mixtures were developed by optimizing aggregate particle packing and conducting overall performance evaluation. This evaluation was carried out in three phases. The first phase investigated the feasibility of new RCMC mixtures by testing workability, compressive strength, and chloride penetrability when cementitious materials content is reduced by 50, 100, and 150 lbs per cubic yard compared to the standard bridge deck concrete mixture of Nebraska. The second phase investigated fresh properties (slump and air content), early-stage properties (setting time and heat of hydration), mechanical properties (compressive strength, modulus of rupture, modulus of elasticity, shear strength, slant shear strength, and bond strength), durability properties (freeze and thaw resistance, and chloride resistivity), and shrinkage properties (free and restrained shrinkage). The third phase investigated the batching, mixing, handling, pumpability, and finishing of the RCMC mixtures by casting mockup deck panels using ready mixed concrete. All the developed RCMC mixtures have demonstrated a comparable performance to the standard mixture while having a reduced cementitious materials content, which is expected to reduce production cost and carbon footprint due to the lower cement content.

17. Key Words	18. Distribution Statement
Low-Cement Concrete, Bridge Deck Cracking, Early-Age Shrinkage, Aggregate Optimization.	

19. Security Classification (of this report)	20. Security Classification (of this page)	21. No. of Pages	22. Price
Unclassified	Unclassified	95	

Form DOT F 1700.7 (8-72) Reproduction of completed page authorized

Disclaimer

The contents of this report reflect the views of the authors, who are responsible for the facts and the accuracy of the information presented herein. The contents do not necessarily reflect the official views or policies neither of the Nebraska Department of Transportations nor the University of Nebraska-Lincoln. This report does not constitute a standard, specification, or regulation. Trade or manufacturers' names, which may appear in this report, are cited only because they are considered essential to the objectives of the report.

The United States (U.S.) government and the State of Nebraska do not endorse products or manufacturers. This material is based upon work supported by the Federal Highway Administration under SPR-FY22(001). Any opinions, findings and conclusions or recommendations expressed in this publication are those of the author(s) and do not necessarily reflect the views of the Federal Highway Administration.

This report has been reviewed by the Nebraska Transportation Center for grammar and context, formatting, and Section 508 compliance.

Acknowledgements

The authors would like to thank the Nebraska Department of Transportation (NDOT) for sponsoring this research project. Special thanks go to the Technical Advisory Committee (TAC) members for their valuable input and guidance throughout this work. The author would also like to thank the materials suppliers: Ash Grove Cement Company, Lyman-Richey Corporation, BASF, EUCLID Chemical, and Master Builders Solutions for the kind donation of materials for this research. Furthermore, the author is also grateful to the UNL graduate students: Dulitha Fredric, Temirlan Barissov, and Mohammed Hedia for their assistance in the experimental investigation.

Table of Contents

List of Figures

List of Tables

Chapter 1 Introduction

1.1 Background

According to the United States (US) Federal Highway Administration (FHWA)'s National Bridge Inventory (NBI) database of 2022, 36% of U.S. bridges need repair work and 3% (5,920) need deck repair or replacement. A common cause of concrete bridge deck and rail deterioration is early-age shrinkage cracking, primarily attributed to the drying shrinkage of restrained concrete (Deng et al., 2016). These cracks commonly occur immediately after construction and even before the bridge is open to traffic. The cracks are primarily in the transverse direction (perpendicular to traffic), with some longitudinal and diagonal cracks at the deck ends. The cracks accelerate the penetration of water, chemicals, and other impurities into the concrete, which leads to reinforcement corrosion, delamination, and eventually concrete spalling. This common deterioration problem results in shorter service life, road closures, and costly repairs and replacements. Figures 1.1 and 1.2 show examples of drying shrinkage cracks in the deck and rail of a newly constructed bridge. These cracks are usually perpendicular to the retrained direction of the component and start early on as narrow and shallow cracks but continue to increase in width and depth as shrinkage increases with time.

Figure 1.1 Early-age shrinkage cracks in bridge decks

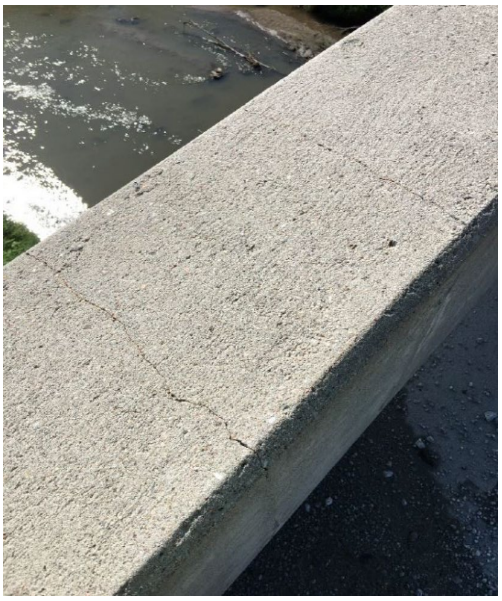

Figure 1.2 Early-age shrinkage cracks in bridge rails

The extent of concrete shrinkage and degree of restraint is dependent on several types of factors such as material, design, and construction (Deng et al., 2016). The focus of this study is on the material factors, particularly the cementitious materials content. A study conducted by Almusallam et al. (1998) presented that use of higher cement content increases the total amount of cracks in concrete as shown in Figure 1.3. A lower rate of evaporation and bleeding was noted in the lab concrete mix made with a lower cement content that minimizes plastic shrinkage cracking. Lower cement content means a lower hydration reaction that helps to keep the concrete temperature low and generate less evaporation.

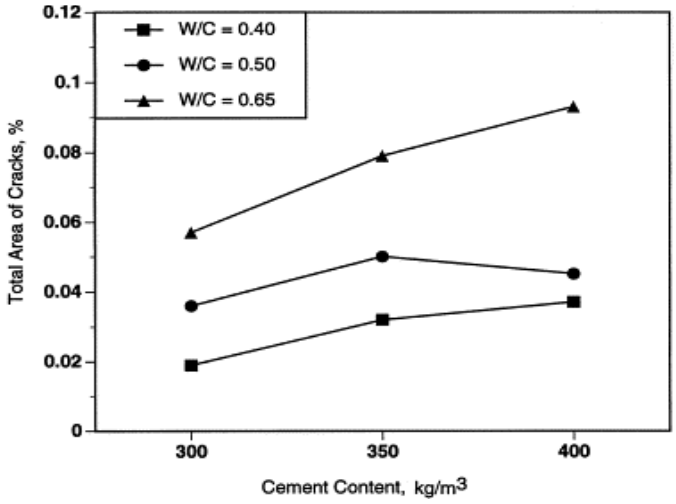

Figure 1.3 Relationship between cement content and total area of cracks (Almusallam et al., 1998)

Xi et al. (2001) at the University of Colorado performed four different lab tests (compressive strength, rapid chloride penetration, crack resistance, and drying shrinkage) to investigate the bridge deck cracking of concrete. Outcomes show the propagation of cracks starts at an early age in concrete with higher cement content when it is too weak and restrained as shown in Figure 1.4. Increasing the coarse aggregate percentage of total aggregate content was also found to increase concrete cracking resistance.

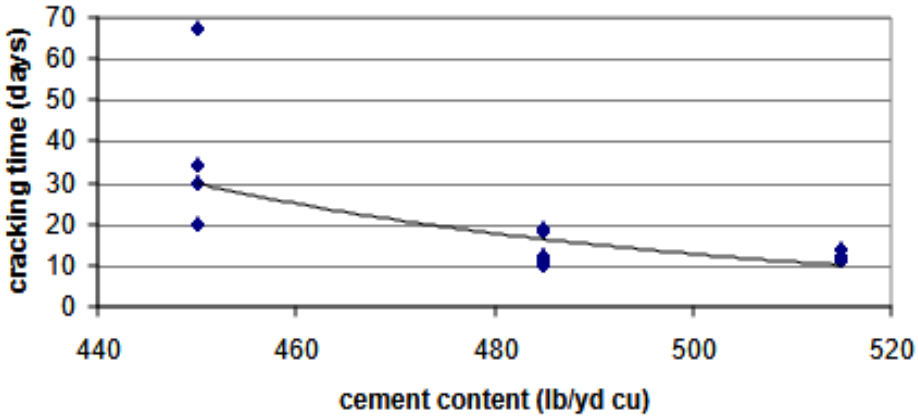

Figure 1.4 Relationship between cracking time and cement content (Xi et al., 2001)

Khajehdehi and Darwin (2018) from the University of Kansas surveyed cracks of 40 monolithic composite bridge decks using the methods developed by Schmitt and Darwin (1995). The 56-days free shrinkage laboratory test data and 96-months crack density data from the 40-bridge survey versus bridge deck concrete paste volume are presented in Figure 1.5 and 1.6, respectively. Paste volume (i.e. the volume of cement, supplementary cementitious materials, and water) was found to be the dominant factor affecting shrinkage and cracking of concrete within the studied range of bridges. Therefore, it is evident that the use of high cementitious materials content increases the rate of shrinkage and the total area of cracking.

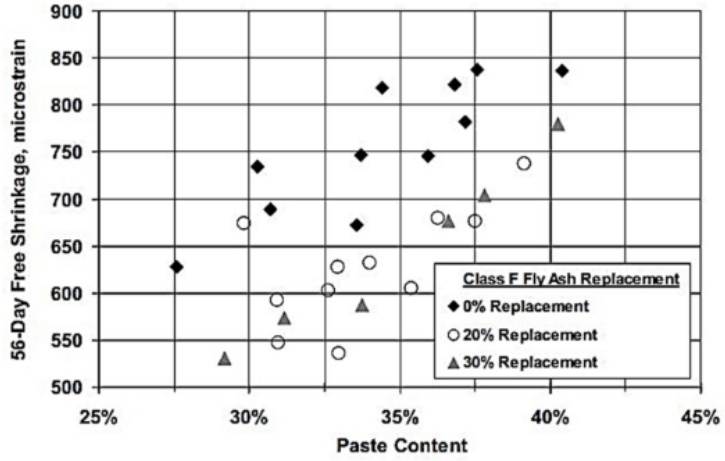

Figure 1.5 56-days free shrinkage vs. paste content for a series of control and replacement of fly ash with cement mix (Khajehdehi and Darwin, 2018)

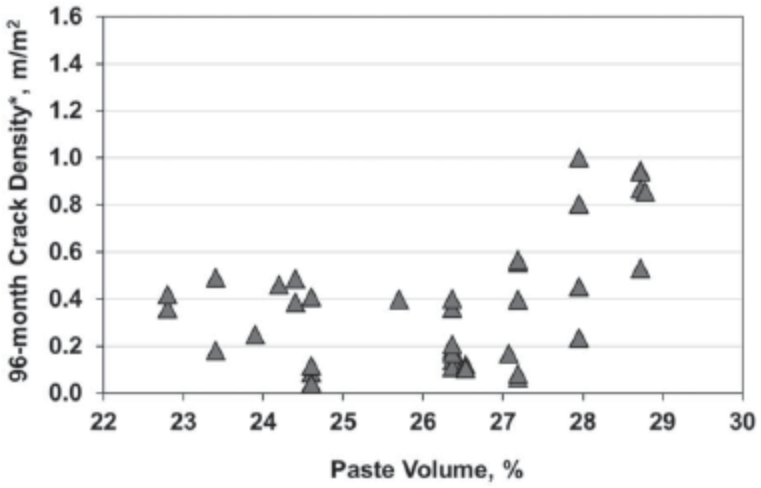

Figure 1.6 Ninety-six-months crack density vs. paste content of concrete decks (Khajehdehi and Darwin, 2018)

Nebraska Department of Transportation (NDOT) currently requires at least seven sacks of cementitious materials (IP/IT) (658 lb) per cubic yard and a minimum compressive strength of 4000 psi for bridge decks and rail concrete mixtures (known as 47BD) as shown in Table 1.1 (outlined in red) (NDOT Bridge Deck specification, Table 1002.02). Type IP cementitious materials is defined by Portland cement with 25% Class F fly ash or Class N pozzolan, and type IT is defined as Portland cement with 40% replacement with slag cement in the specification (section 1004.02). Despite the recently improved NDOT curing requirements of bridge decks (10-day wet curing followed by 7-day curing compound), early-age shrinkage cracking is still a concern. Based on the outcomes of a recently completed NDOT funded research project (Report No SPR-P1(18) M069) conducted to reduce cementitious materials content in pavement concrete, the aggregate packing optimization approach is proposed to reduce cementitious materials content in the 47BD concrete mixture while meeting the strength requirements for bridge decks and rails. In addition, workability, mechanical, viscoelastic, durability, and pumpability properties, need to

be evaluated to ensure the constructability and overall performance of the new reduced-cementitious materials concrete (RCMC) mixtures.

Table 1.1 NDOT Concrete Mixtures' Characteristics (NDOT Standard specification, Table 1002.02)

Class of Concrete (1)	Base Cement Type	Total Cementitious Materials Min. lb/cy	Total Aggregate	
			Min. lb/cy	Max. lb/cy
47B**		564	2850	3150
47B***		564	2850	3150
47BD	IP/IT*	658	2500	3000
47B-HE		752	2500	3000
$BX_{(4)}$		564	2850	3150
47B-OL****		564	2850	3200
PR1	I/II	752	2500	2950
PR3	III	799	2500	2950
$SF_{(5)}$	I/II	589	2850	3200

Table 1002.02 (Continued)

Class of Concrete (1)	Air Content % Min.-Max. (2)	Ledge Rock (%)	Water/ Cement Ratio Max. (3)	Required Strength Min. psi
47B**	6.5 -9.0	-	0.45	3500
47B***	6.0 - 8.5	-	0.45	3500
47BD	6.0 - 8.5	30+3	0.42	4000
47B-HE	6.0 - 8.5	30±3	0.40	3500
$BX_{(4)}$	6.0 - 8.5	-	0.45	3500
47B-OL****	5.0-7.0	30±3	0.36	4000
PR1	6.0 - 8.5	30±3	0.36	3500
PR3	6.0 - 8.5	30±3	0.45	3500
$SF_{(5)}$	6.0 - 8.5	50±3	0.36	4000

1.2 Research Objective

The main objective of this research is to develop reduced-cementitious material content concrete mixtures for bridge decks and rails that minimize early-age shrinkage cracking. This was accomplished by optimizing aggregate particle packing and experimentally evaluating the overall performance of the newly developed mixtures. Aggregate packing optimization of locally available materials in East Nebraska using the Modified Toufar Model and Combined Aggregate Void Content test was conducted (Mamirov et al., 2019). The experimental program was done in three phases: preliminary-investigation, comprehensive experimental investigation, and large-scale demonstration. Expected outcomes are reduction of early-age shrinkage cracking, increased service life of bridge decks and rails, and minimized road closures and detours associated with repair and replacement activities. In addition, the use of less cementitious materials in bridge construction will reduce the construction cost and carbon footprint, which have significant economic and environmental advantages.

1.3 Organization of the Report

The project report contains six chapters. Chapter 1 is an introduction where the background, objectives, and significance of this research project are stated. Current practice of other Midwest states for bridge deck concrete are presented in Chapter 2 as a part of the literature review along with some other available research studies for reducing shrinkage cracking. Chapter 3 presents the properties of materials used in the study, concrete mixing procedures, and test methods. Results of the preliminary and comprehensive experimental investigations are presented as the performance evaluation in Chapter 4, where the feasibility of reduced cementitious materials concrete (RCMC) is determined by testing all fresh, early-age, mechanical, and long-term durability properties of concrete. Chapter 5, the production mockup,

involves the production and testing of the lab-scale bridge deck slabs to demonstrate the batching, pumpability, and constructability of the new mixtures. Lastly, Chapter 6 presents a summary of the research conclusions and recommendations.

Chapter 2 Literature Review

2.1 Overview

Several methods are available for limiting early-age cracking of concrete bridge decks made by conventional Portland cement concrete (PCC). Reduction of cementitious materials content accomplished with optimization of aggregate gradation in the concrete mixture (Lindquist, 2008), use of pre-wetted fine lightweight aggregate (LWA) for internal curing (Abdigaliyev et al., 2020), the addition of shrinkage reducing admixture (SRA) or expansive cement (Type K) with LWA (Ardeshirilajimi et al., 2016), and use of glass and nylon fibers (Khan et al., 2016) are notable among them. Some methods are already being implemented to some extent by several state DOTs and others are only experimental outcomes. This report focuses mainly on the reduction of cementitious materials content in concrete mixtures with aggregate optimization for concrete bridge decks and rails to reduce early age bridge deck cracking. The available investigations conducted by several state DOTs on reduction of cementitious materials content in bridge decks are also presented.

2.2 State DOT Current Practice and Specifications

To compare the current cementitious materials content in Nebraska bridge decks and rail with that in other states, 14 states (11 Midwest states and 3 others—Wyoming, Colorado, and Nevada) bridge deck concrete specifications were summarized in Table 2.1

Table 2.2 State DOTs current practice for bridge deck concrete

State (Year)	Cement Type	Cement Content (lb/cy)	Cementitious Materials (CM) (lb/cy)		Water /CM ratio	Slump (inch)		Air Content (%)		Coarse Aggregate		Compressive Strength (psi)		Curing	Notes
										Nominal size	Max. Size				
	-	Min.	Min.	Max.	Max.	Min.	Max.	Min.	Max.	(Sieve No.)	(Inch)	Min.	days	Min.	-
Nebraska (2017)	IP/IT	N/A	658	N/A	0.42	N/A	N/A	6.0	8.5	N/A	1.5	4000	28	10-day moist followed by 7-day membrane	
Kansas (2015)	IP/IS/IT/II	N/A	480	N/A	0.45	N/A	5.0	5.0	8.0	N/A	1.5	4000	28	With overlay:14-day wet. Without overlay: 14-day wet followed by 7-day membrane	-
South Dakota (2015)	II	585 (*565)	N/A	800	0.45	2.0	4.0	5.0	7.5	N/A	1.5	4000	28	Immediate fog and 7-day wet.	*if well-graded aggregate used
		650 (*615)										4500	28		
		715 (*680)										5000	28		
Illinois (2016)	I/II	605	N/A	N/A	0.44	2.0	4.0 (*7.0)	5.0	8.0	N/A	1.5	4000	14	7-day wet.	* with HRWR
Minnesota (2020)	I/II/IS/IL/IP	N/A	N/A	750	0.45	2.0	4.0	5.0	8.5	# 67	N/A	4000	28	7-day wet	-

State (Year)	Cement Type	Cement Content (lb/cy)	Cementitious Materials (CM) (lb/cy)		Water /CM ratio	Slump (inch)		Air Content (%)		Coarse Aggregate		Compressive Strength (psi)		Curing	Notes
										Nominal size	Max. Size				
	-	Min.	Min.	Max.	Max.	Min.	Max.	Min.	Max.	(Sieve No.)	(Inch)	Min.	days	Min.	-
Missouri (2019)	N/A	517	N/A	N/A	0.40	N/A	3.0	4.5	7.5	N/A	1.0	4000	28	7-day wet and until 3000 psi strength	-
Wisconsin (2022)	I/II	500	565	N/A	0.45	1.0	4.0	4.5	7.5	N/A	1.0	4000	28	7-day wet followed by coated membrane	-
Indiana (2020)	N/A	564	N/A	800	0.45	N/A	N/A	5.0	8.0	N/A	1.0	4000	28	7-day wet and until 550 psi flexural strength	-
Michigan (2020)	I/II	N/A	517	658	0.45	N/A	7.0	5.5	8.5		1.5	4500	28	Single coat curing compound followed by 7-day wet	-
Colorado (2019)	N/A	N/A	500	640	0.44	Design slump -2	Design Slump + 2	5.0	8.0	#57	1.5	4500	56	7-day wet	-

State (Year)	Cement Type	Cement Content (lb/cy)	Cementitious Materials (CM) (lb/cy)		Water /CM ratio	Slump (inch)		Air Content (%)		Coarse Aggregate		Compressive Strength (psi)		Curing	Notes
										Nominal size	Max. Size				
	-	Min.	Min.	Max.	Max.	Min.	Max.	Min.	Max.	(Sieve No.)	(Inch)	Min.	days	Min.	-
Wyoming (2021)	II	611 (*489)	N/A	N/A	0.45	N/A	6.0	4.5	7.5	N/A	1.5	4000	28	5-day wet or curing compound	*mixing with fly ash
Ohio (2019)	I/II	N/A	520	N/A	N/A	2.0	4.0 (*7.0)	5.0	9.0	N/A	N/A	4000	28	7-day wet followed by coated membrane	-
		N/A	520	N/A	N/A					N/A	N/A	4500	28		-
		N/A	520	N/A	N/A					N/A	N/A	As per plan	N/A		*by adding chemical admixture
North Dakota (2020)	II	N/A	600	650	0.44	1.0	3.0	5.0	8.0	N/A	1.5	4000	28	7-day wet (*10-day wet)	*if more than 10% cement replaced by pozzolans
Iowa (2015)	I/II/IS/ IP	N/A	N/A	N/A	0.488	1.0	5.0	5.5	8.5	N/A	1.5	4000	28	4-day for class C concrete. 7-day for class HPC. Either white pigment or moist.	-

State (Year)	Cement Type	Cement Content (lb/cy)	Cementitious Materials (CM) (lb/cy)		Water /CM ratio	Slump (inch)		Air Content (%)		Coarse Aggregate		Compressive Strength (psi)		Curing	Notes
										Nominal size	Max. Size				
	-	Min.	Min.	Max.	Max.	Min.	Max.	Min.	Max.	(Sieve No.)	(Inch)	Min.	days	Min.	-
Nevada (2014)	II/V/IP	564	N/A	N/A	0.40	0.50	4.00	4.0	7.0	N/A	1.00	As per plan	N/A	10-day wet followed by 7-day curing compound	
	Average	550	542	716	0.44	1.44	4.5	4.97	8.0		1.35	4176.50			
	Std. Dev.	42	56	76	0.03	0.62	1.27	0.48	0.53		0.24	303			

NDOT requires one of the highest cementitious materials (cm) content (658 lb/cy) among Midwestern state DOTs. NDOT cementitious materials content is 37% higher than the minimum requirement of the Kansas Department of Transportation (KDOT) (480lb/cy) and 20% higher than the average requirement for the remaining DOTs. The low content of cementitious materials of KDOT is possible when using their own optimized mixed aggregate gradation. On the other hand, the highest maximum water-cementitious materials (w/cm) ratio is that of the Iowa DOT (0.49) and the lowest is that of the Missouri DOT (0.40). NDOT specifies a w/cm of 0.42 and requires a 10-day wet curing period followed by a 7-day membrane curing. Other NDOT requirements include slump (average 1.44 - 4.50), air content (average 4.97 - 8.0 %), maximum coarse aggregate size (1.0-1.5 inch), and the minimum 28 days compressive strength of concrete (4000-4500 psi), which differ from the requirements of other DOTs.

2.3 State DOT Research

Lindquist et al. (2008) developed a mix with optimized aggregate gradation for bridge decks in Kansas to reduce early age shrinkage cracks. The shrinkage factors of 14 LC-HPC (low cracking – high-performance concrete) bridge decks in Kansas were monitored over one year. All mixtures of this study had paste volumes of less than 24.4% with the optimum grade aggregate as shown in Table 2.2. A total of 535-540 lb/cy Type I/II cement with a water-cement ratio of 0.44 to 0.45 were used. Although the required compressive strength of concrete was 4000 psi, 3790 to 6380 psi (26.1 to 44.0 MPa) strength was found with LC-HPC. Figure 2.1 shows the retained percentage chart and Figures 2.2 and 2.3 show the Modified Coarseness Factor Chart (MCFC) used for determining the optimum combination and its effect on workability.

Table 2.3 Combined aggregate gradation for LC-HPC (Lindquist et al., 2008)

Usage	Percent Retained on Individual Sieves – Square Mesh Sieves*									
	25.0 mm (1")	19.0 mm (3/4")	12.5 mm (1/2")	9.5 mm (3/8")	4.75 mm (No. 4)	2.39 mm (No. 8)	1.18 mm (No. 16)	600 µm (No. 30)	300 µm (No. 50)	150 µm (No. 100)
Bridge Deck	2-6	5-18	8-18	8-18	8-18	8-18	8-18	8-15	5-15	0-5
Corral Rails	0	2-6	8-20	8-20	8-20	8-20	8-20	5-15	5-15	0-6

*The maximum allowable percentage passing the 75 µm (No. 200) is 2.5%.

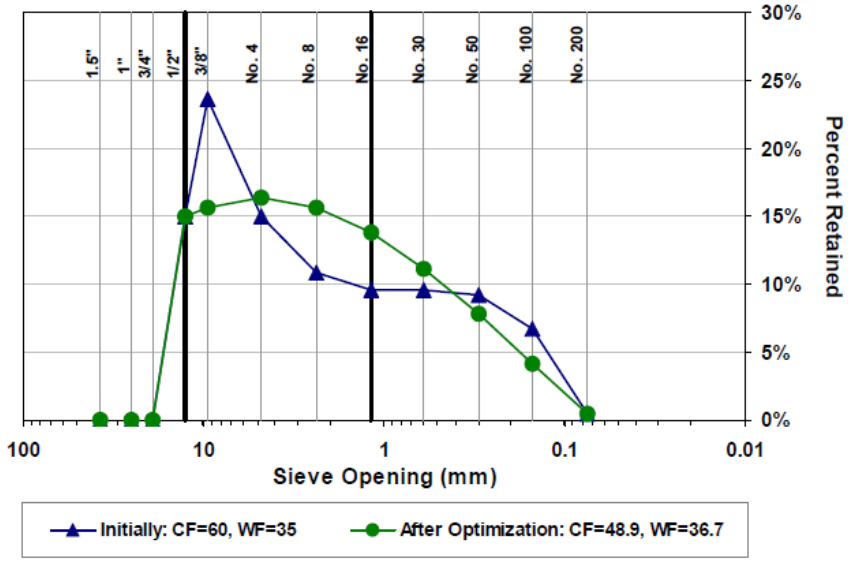

Figure 2.1 Cubic-Cubic Model of optimized gradation plotted on a percent retained chart (Lindquist, W.D., 2008)

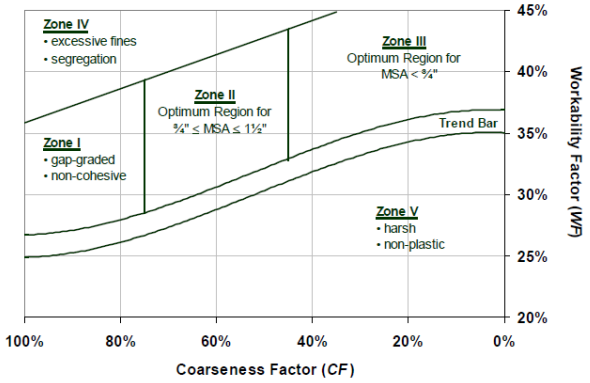

Figure 2.2 Modified coarseness factor chart (MCFC) (Lindquist, W.D., 2008)

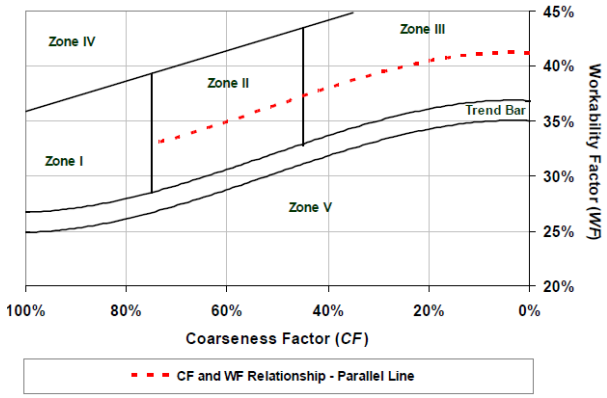

Figure 2.3 Relationship between the coarseness factor and workability factor plotted on the Modified Coarseness Factor Chart (MCFC) (Lindquist, W.D., 2008)

Investigation on shrinkage was performed in six phases (Lindquist et al., 2008). Phase one indicated that reduction in water-cement (w/c) ratio by reducing water content with an equal volume of aggregate and maintaining workability with a high-range water reducer (HRWR) does not increase shrinkage, while a longer curing period (≥ 14 days) reduces concrete shrinkage. Observation of the second phase indicated the opposite, which concludes that concrete with a higher w/c ratio exhibits less shrinkage than concrete with a lower w/c ratio. Phase three indicated that increasing curing time has little effect on the shrinkage of concrete containing quartzite or granite but a significant effect on limestone mixtures. All other parameters were kept constant in this phase. Phase four denoted that the addition of shrinkage reducing admixture (SRA doses, 0 – 2 %) decreases early age shrinkage but increases long-term drying shrinkage. According to phase five, increased curing time reduces shrinkage for Type II, Type I/II, and Type III cement. Phase six indicated that high absorption coarse aggregate (such as limestone) with 0 – 6% silica fume does not affect shrinkage much, but low absorption coarse aggregate increases early age shrinkage with 3 – 6 % silica fume. Among 14 LC-HPC bridges, four have a very high cost, six have a moderately high cost, and two cost less than the control deck (Lindquist et al., 2008).

Qiao et al. (2010) investigated several bridges in Washington and recommend the optimization of concrete mix design as an appropriate mitigation strategy for early age bridge deck cracks. Twenty concrete mixes were designed and compared with two existing WSDOT concrete mixes as a benchmark. It was found that the use of a shrinkage-reducing admixture (SRA) reduces the shrinkage and increases both flexural and compressive strength of concrete. Adding fly ash as a partial replacement of Portland cement decreases the concrete early-age strength which may initiate cracks earlier. The moderate use of silica fume (6-8% of c-m mass) with 7 days of continuous curing was recommended to limit the shrinkage. Aggregate sizes 1.5 inches, 2.0 inches, and 2.5 inches were tested from two different sources. Both the size and source of coarse aggregates influenced the concrete strength. Use of a larger size aggregate with less paste volume was recommended. Due to the flexibility of coarse aggregate size in the "KU Mix" design, it was used along with ACI 211.1-91 guidelines for mix design. With the reduction of cementitious materials paste content, the high range water reducing admixture was also used to maintain workability. Although all 28 mixes fulfill the WSDOT minimum compressive strength requirement of 4000 psi in 28 days, a larger size aggregate (2 in. or 2.5 in.) showed a reduced strength property with better shrinkage resistance.

Wan et al. (2010) performed laboratory and field studies of 16 bridges in Wisconsin along with analytical and finite element analyses to investigate new concrete bridge deck cracking problems. Fifteen bridge structures were analyzed analytically using 21 variables and 16 were investigated through visual inspection to identify the cause of cracking. Observations indicated that a longer curing period and waiting until the concrete gets older to open the bridge superstructure to traffic proved to be beneficial in preventing early age cracking. In addition, simply supported decks were encouraged over continuous decks to prevent cracking. According

to investigations in the literature review, the following are measures that can be taken to prevent early-age cracking:

- Curing compounds as quickly as possible.
- Limiting the amount of cement to 600 lb/yd^3.
- Limiting w/c ratio by 0.4.
- Controlling the volume of cement and water by 27.5%.
- Holding air content less than 6%.
- The theoretical evaporation rate should not exceed 0.25 lb/ft^2/hr.
- Pouring the concrete in the positive moment region of the deck first and ensuring the pouring ratio is not less than 0.6 span lengths/hr.
- The clear cover for top reinforcement should be 2.5 inches.

Xi et al. (2001) proposed three mix designs to use in summer, winter, and only for thin overlay to mitigate the cracking problem of bridge decks in Colorado. The goal was to achieve 4500 psi compressive strength, 6.5% air content, and a 3-4-inch slump with a maximum aggregate size of ¾ inch. These mixes had a reduced cementations materials content of more than 100 lb/yd^3 while maintaining the required workability. Moreover, it was found that Class F fly ash reduces the permeability compared to Class C fly ash and makes the concrete more durable. Also, it was concluded that a larger aggregate size and a higher proportion of gravel helps to resist cracking more than the intermediate size. Finally, it was proposed to use concrete with 465 to 485 lb/yd^3 cement content, a w/cm ratio of 0.37 to 0.41, Class F fly ash of 20-25%, and seven days of curing time for bridge decks. The performance of the developed mixes was not evaluated in any real projects when the report was published.

Caltrans (California DOT) studied the early-age bridge deck cracks of California and recommended the following solutions:

- Maximum cementitious content of 600 lb/yd^3 and paste content of 27% by volume.
- Larger aggregate size, at least 1-inch for nominal maximum aggregate size.
- Apply wet curing as soon as possible (roughly within 10-20 minutes).
- Prohibit silica fume in deck concrete and increase the curing period of concrete with fly ash to a minimum of 21 days.
- Air entrainment of 6-8%.
- Internal curing is encouraged.
- Reduce the maximum free shrinkage limit to 0.040% in 28 days.
- Cast in situ w/cm ratio of 0.43-0.45.
- Maximum penetration of two inches and maximum slump of four inches. Allow penetration up to 2.5 inches if superplasticizer is used.
- Use of cement Type II instead of III.
- Place deck during late afternoon in hot weather (such as Summertime).
- Simply supported decks instead of continuous span.

Chaunsali et al. (2013) investigated the application of expansive cement (Type K and Type G) and shrinkage-reducing admixtures (SRAs) to reduce the drying shrinkage cracking of bridge decks in Illinois. The Type K expansive cement contains Portland cement and calcium sulfa-aluminate-based components whereas the Type G expansive cement was made of Portland cement and CaO-based components. Although both Type K and Type G concrete strength was comparable to the control concrete mix, the expansion rate of Type G concrete was faster than Type K concrete, presented in Figure 2.4 and 2.5. Mineral admixtures such as Class F fly ash increased expansion in both expansive concretes (with Type K and Type G), whereas silica fume reduced the extent of expansion. The addition of Class C fly ash initially increased expansion, but expansion stopped earlier than usual in the Type K-based mix. An increase in SRA dosage

was found to increase the time before cracking occurred, but it also reduced compressive strength. The possibility of a heated girder creating cracks in the concrete deck was also investigated using the SAP2000 and Abaqus models.

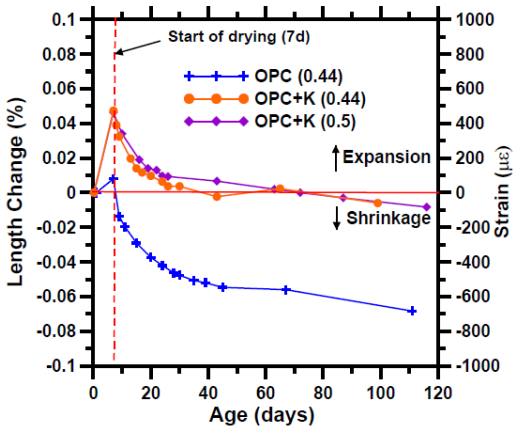

Figure 2.4 Expansion and shrinkage characteristics of Type K concrete in comparison with ordinary Portland cement concrete (Chaunsali et al., 2013)

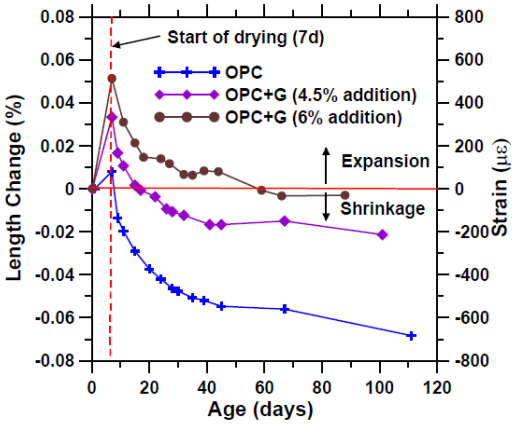

Figure 2.5 Expansion and shrinkage characteristics of Type G concrete in comparison with ordinary Portland cement concrete (Chaunsali et al., 2013)

Ardeshirilajimi et al. (2016) studied the effect of pre-soaked lightweight aggregates (LWA) to minimize the young age cracking of concrete in Illinois. It is determined that although LWA can significantly reduce autogenous shrinkage, its effect on drying shrinkage is minimal and, in some cases, could adversely increase the drying shrinkage. Moreover, the combined effects of LWA and expansive cement (Type K), and LWA and shrinkage-reducing admixtures (SRAs) on drying shrinkage are also studied. It has been shown that the addition of Type K cement or SRA to mixtures containing LWA can significantly reduce drying shrinkage and make the mixture more volumetrically stable.

Khan and Ali (2016) pointed out that high use of cement content to achieve high compressive strength is the main cause of early-age cracking of concrete. They proposed adding 50 mm fibers made of glass and nylon to concrete during mixing (named GFRC and NFRC,

respectively). Although assuredly this change reduced early-age cracking with the increase of concrete tensile strength, the compressive strength was compromised up to 6% and concrete production cost increased with the fiber additions.

To address the early-age premature cracks in Nebraska bridge decks, Abdigaliyev et al. (2020) came up with internal curing by using light weight fine aggregates (LWFAs) in replacement of conventional fine aggregate (sand and gravel) in Nebraska. It was stated that a 28-day higher compressive strength, lower curing period, low chloride ion penetrability and reduction in autogenous shrinkage was possible with the LWFAs mixture even though workability and early-age low resistivity was still an issue.

Chapter 3 Materials and Methodology

3.1 General

Materials used in this research and the test methods conducted to evaluate concrete properties are described in this chapter. Properties of the typically used materials for concrete bridge decks in Nebraska (i.e., IPF cement, limestone, and sand and gravel) are presented. Test procedures to evaluate concrete fresh, early-stage, and hardened properties are also described. All the materials used in this study comply with the Nebraska DOT standard specifications of materials approved for bridge deck construction.

3.2 Materials

3.2.1 Cement and Cementitious Materials

NDOT Standard Specifications for Highway Construction (2017) requires the use of IP blended cement for bridge application. Type IP Portland-pozzolan cement with 25% blended class F fly ash content that meets ASTM C595 "Standard Specification for Blended Hydraulic Cement" (ASTM 2019) was used as the cementitious material in this study. The chemical composition and physical properties of the cementitious materials are reported in Table 3.1.

Table 3.4 Chemical composition and physical properties of IP cement

Chemical Properties	Pozzolan content, %	25.00
	MgO, %	2.45
	SO_3, %	3.10
	Loss in Ignition, %	1.00
Physical Properties	Blaine Fineness, cm^2/g	4,400
	Specific Gravity	2.95

3.2.2 Aggregates

Figures 3.1 and 3.2 show the locally available limestone (LS), and sand and gravel (SG), respectively, commonly used in Nebraska for concrete bridge decks and rails. Aggregate from Eastern Nebraska (Omaha area) was used in this research. Before every mix, aggregates were collected in plastic buckets, weighted to the batch quantity, and covered with a lid. Moisture content was calculated before every mix measuring the weight of the aggregate sample before and after oven drying.

$$\text{Moisture Content (\%)} = (W_{AD} - W_{OD})/ W_{AD} * 100$$

Where,

W_{AD} = Weight of aggregate in air-dry condition

W_{AD} = Weight of aggregate in oven-dry condition

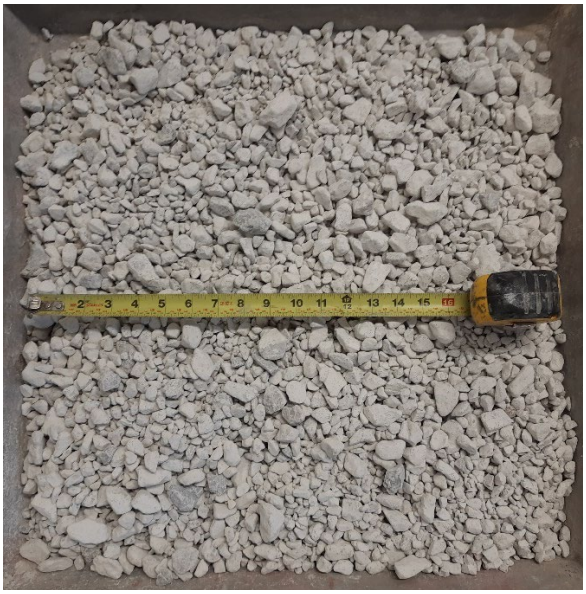

Figure 3.1 Limestone (LS)

Figure 3.2 Sand and Gravel (SG)

Specific gravity and absorption at saturated surface dry (SSD) condition of coarse and fine aggregates were obtained in accordance with ASTM C127 and ASTM C128, respectively. The obtained values along with the fineness modulus (FM) are presented in Table 3.2.

Table 3.5 Aggregate properties

Aggregate Type	Specific Gravity	Absorption (%)	Fineness Modulus (FM)	Nominal Maximum Aggregate Size (in.)
SG	2.586	0.96	3.86	-
LS	2.671	0.91	6.99	1.00

Sieve analysis data of SG and LS are presented in Table 3.3 and Table 3.4, respectively, while the gradation curves are plotted in Figure 3.3.

Table 3.6 Gradation of Sand and Gravel (SG)

Sieve Number	Sieve Opening (mm)	Sieve Opening (inch)	Aggregate Retain (lbs.)	Cumulative Retain (lbs.)	% Retain	% Passing
1.5"	37.500	1.5000	0.00	0.00	0.00	100.00
1"	25.000	1.0000	0.00	0.00	0.00	100.00
3/4"	19.000	0.7500	0.06	0.06	0.93	99.07
1/2"	12.500	0.5000	0.11	0.17	2.57	97.43
3/8”	9.500	0.3750	0.15	0.32	4.84	95.16
#4	4.750	0.1870	0.63	0.95	14.38	85.62
#8	2.360	0.0937	1.08	2.03	30.77	69.23
#16	1.180	0.0469	1.47	3.49	53.03	46.97
#30	0.600	0.0234	1.33	4.83	73.23	26.77
#50	0.300	0.0117	1.21	6.03	91.54	8.46
#100	0.150	0.0059	0.47	6.50	98.69	1.31
#200	0.075	0.0029	0.07	6.57	99.77	0.23
Pan	-	-	0.02	6.59	-	-
		Total	6.59			

Table 3.7 Gradation of Limestone (LS)

Sieve Number	Sieve Opening (mm)	Sieve Opening (inch)	Aggregate Retain (lbs.)	Cumulative Retain (lbs.)	% Retain	% Passing
1.5"	37.500	1.5000	0.00	0.00	0.00	100.00
1"	25.000	1.0000	0.06	0.06	0.26	99.74
3/4"	19.000	0.7500	1.66	1.72	7.79	92.21
1/2"	12.500	0.5000	6.12	7.84	35.57	64.43
3/8”	9.500	0.3750	5.10	12.94	58.70	41.30
#4	4.750	0.1870	7.64	20.58	93.37	6.63
#8	2.360	0.0937	0.92	21.49	97.53	2.47
#16	1.180	0.0469	0.11	21.61	98.04	1.96
#30	0.600	0.0234	0.07	21.68	98.37	1.63
#50	0.300	0.0117	0.14	21.82	99.00	1.00
#100	0.150	0.0059	0.22	22.03	99.98	0.02
#200	0.075	0.0029	0.00	22.04	100.00	0.00
Pan	-	-	0.00	22.04	-	-
		Total	22.04			

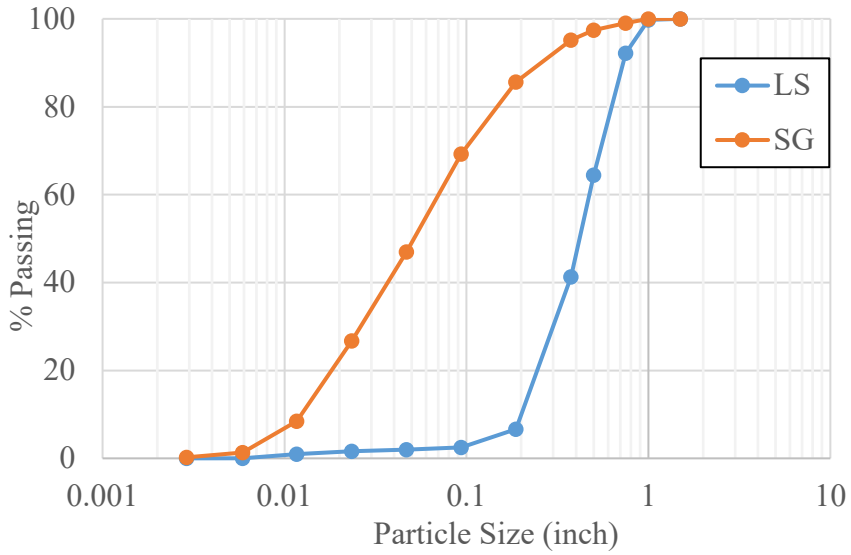

Figure 3.3 Aggregate gradation curves

3.2.3 Chemical Admixtures

A commercially available air-entraining admixture that meets the requirements of ASTM C260 (Standard Specification for Air-Entraining Admixtures for Concrete) was used as an air-entraining agent (AEA). A mid-range water reducer that meets the requirements of ASTM C494

(Standard Specification for Chemical Admixtures for Concrete) was used as the water-reducing (WR) agent for all mixes.

3.3 Aggregate Packing Optimization

The most common approach to reducing cementitious materials content is to improve the particle packing of the aggregate skeleton which consists of particle fractions of different sizes, shapes, and textures. In general, aggregates occupy around 70-80% of the concrete mixture by volume. Optimization of particle packing implies achieving as dense a matrix as possible, i.e., with the lowest possible voids in between particles. The lower the volume of voids, the less cementitious materials paste is needed to fill them as shown in Figure 3.4. Aggregates used in Eastern Nebraska were investigated by Miras et al. (2021) to find the optimized blend. First, optimum aggregate blends were identified using the Modified Toufar Model, which later indicated a good correlation with the experimental packing results based on the combined void content test. Among all the packing degrees investigated, 55SG-45LS was recommended as the optimized blend. This combination's aggregate is 55% SG and 45% LS. This 55SG-45LS aggregate combination ratio was applied to all mixes with necessary adjustments for cementitious materials reductions.

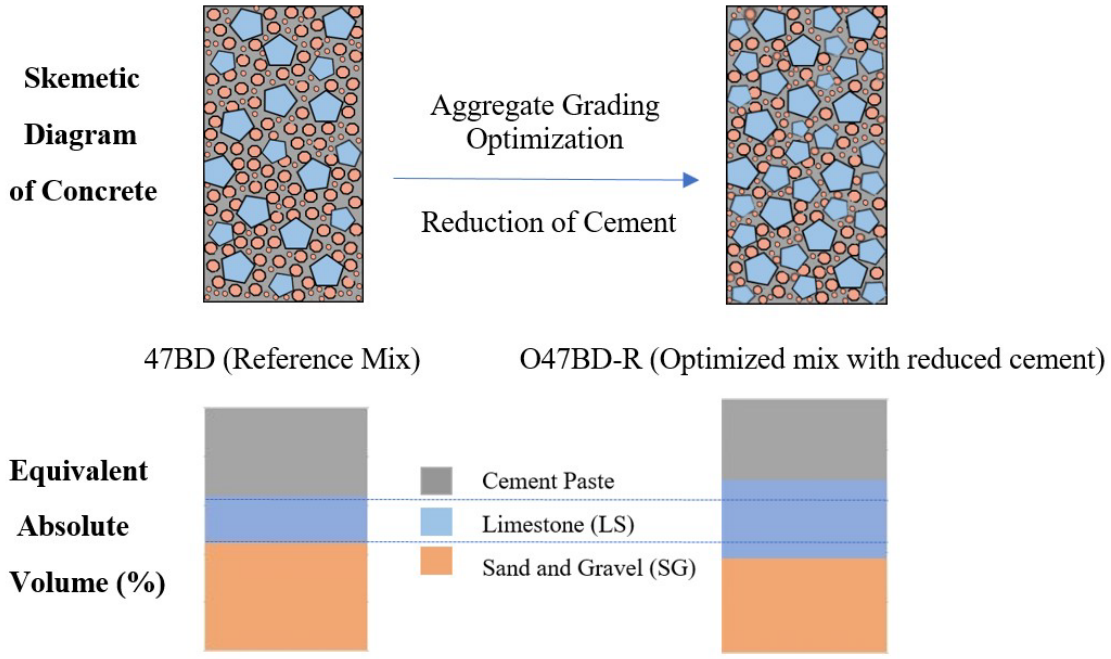

Figure 3.4 Illustration of cementitious materials content reduction through aggregate gradation optimization

3.4 Concrete Mixing

A drum mixer with a 5.5 ft^3 (0.156 m^3) capacity was used to mix small concrete batches (1 – 1.5 ft^3) and a mixer with a 7 ft^3 (0.2 m^3) capacity was used for big batches (2.5 – 2.8 ft^3) following the standard procedure of ASTM C192 (Standard Practice for Making and Curing Test Specimens in the Laboratory). First, the coarse aggregate was mixed with approximately half of the batch water containing AEA for 30 seconds to generate enough entrained air bubbles (Figure 3.5). Then, sand and gravel, cement, and the remaining water with water-reducing admixture were added and mixed for three minutes followed by three minutes of resting and an additional two minutes of mixing. The additional adjustment was made based on the slump and air-content test by adding admixtures or simply waiting. The concrete was mixed for another two minutes after any adjustment was done. Tests conducted from each batch are presented in Table 3.5.

Figure 3.5 Formation of air with limestone

Table 3.8 Test Methods

State	Property	Test Method	Standard/Source
Fresh	Workability	Slump	ASTM C143 (AASHTO T119)
	Unit weight	-	ASTM C138 (AASHTO T121)
	Air content	Pressure method	ASTM C231 (AASHTO T152)
	Workability under vibration	Vibrating L-box	Nevada DOT (Report 366-16-803)
Early-Age	Time of setting	Penetration resistance	ASTM C403 (AASHTO T197)
	Heat of hydration	Isothermal calorimeter	ASTM C1702
Mechanical	Compressive strength	Compression	ASTM C39 (AASHTO T22)
	Modulus of rupture	4-point bending	ASTM C78 (AASHTO T97)
	Modulus of elasticity	-	ASTM C469
	Shear strength	Push-off	Mattock and Hawkins, 1972
	Concrete-Rebar bond strength	Pull-out of horizontal bars	RILEM/CEB/FIB. 1970
	Concrete-Concrete bond strength	Slant shear	ASTM C882
Durability	Freeze-Thaw resistance	Freeze-thaw cycling	ASTM C666
	Surface resistivity	Electrical resistivity	AASHTO TP 95-14
	Chloride ion penetrability	Rapid chloride penetration	ASTM C1202
Shrinkage	Drying shrinkage	Restrained shrinkage	ASTM C1581
		Free shrinkage	ASTM C157 (AASHTO T160)

3.5 Fresh Concrete Properties

Fresh concrete properties were tested immediately after mixing. Temperature, slump, unit weight, air content, and vibrating L-box tests were conducted in this stage.

3.5.1 Temperature

The temperature of fresh concrete was monitored with a temperature probe (Figure 3.6) at the end of every mix before any other test was done according to the ASTM C1064. The probe was inserted three inches inside the concrete for two minutes before recording the temperature.

Figure 3.6 Fresh concrete temperature measurement

3.5.2 Workability

The slump test (Figure 3.7) was done to measure the consistency of concrete according to ASTM C143 (Standard Test Method for Slump of Hydraulic-Cement Concrete). Although slump does not directly measure the workability or water content of concrete, it is a measure of the relative mobility of concrete which could be used as indicators of workability. A slump range of 4.0 - 6.5 inches was considered an acceptable range for the bridge deck mix.

Figure 3.7 Slump test

Figure 3.8 Unit weight measurement

3.5.3 Unit Weight

The unit weight of concrete was measured in a 0.25 ft^3 (Figure 3.8) container following ASTM C138 [Standard Test Method for Density (Unit Weight), Yield, and Air Content (Gravimetric) of Concrete]. The weight of 0.25 ft^3 was then multiplied by 4.0 to get the unit weight of concrete (1 ft^3).

3.5.4 Air Content

Air content was tested according to ASTM C231 (Standard Test Method for Air Content of Freshly Mixed Concrete by the Pressure Method) using a type-B pressure meter (Figure 3.9). An acceptable air content range for the bridge deck mix was 6.0 – 8.5 percent.

Figure 3.9 Air pressure measurement (meter type-B)

3.5.5 Workability Under Vibration

The L-box test was conducted to check the flow of concrete under vibration following the procedures used in the Nevada DOT report no. 366-16-803. The test was done in an L-shaped steel box shown in Figure 3.10. The 4-inch and 6-inch marks were made from the face of the gate to determine the time it takes the mix to flow to each mark.

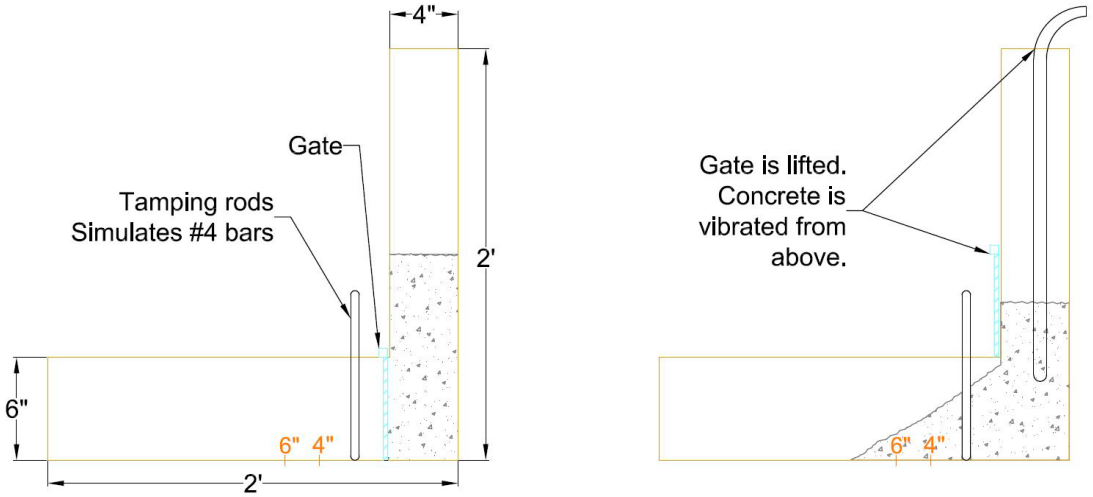

Figure 3.10 Sketch of an L-box with dimensions (left) and test scenario (right) (Nevada DOT report)

A rod was clamped as shown in Figure 3.11 where the horizontal portion of the box replicates concrete passing through a #4 rebar at 3" spacing in a real poring scenario. First, concrete was poured one foot deep in the vertical portion of the L-box without any compaction while the gate was closed. Then, while opening the gate the vibrator was slowly inserted until it reached approximately one inch from the bottom, shown in Figure 3.12. T_4 and T_6 were recorded as the time it takes the concrete to pass the four-inch and six-inch marks shown in Figure 3.13. The total distance the concrete travels from the gate is reported as D_f.

Figure 3.11 L-box setup

Figure 3.12 Insertion of the vibrator in L-box

Figure 3.13 Concrete passing the 6-inch mark under vibration in L-box

3.6 Early-Age Properties

3.6.1 Time of Setting

The initial and final set times of concrete were tested using the penetration method according to ASTM C403 (Standard Test Method for Time of Setting of Concrete Mixtures by

Penetration Resistance). A 6”x6” cylinder was cast with mortar for every mix. Mortar was collected by separating coarse aggregate from concrete using a #4 (4.75 mm opening) wet sieve. The specimen shown in Figure 3.14 was cast in one layer and consolidated by tamping 28 times (1 tamping/square-inch). The resisting force to penetrate one inch of the test needle in concrete was recorded with time and letter plotted with a resistance-time curve. The time required for concrete to resist 500 psi and 4000 psi of force was reported as initial and final set times, respectively.

Figure 3.14 Penetration resistance test for concrete set time

3.6.2 Heat of Hydration

The heat of hydration test was done according to ASTM C1702 (Standard test method for measurement of heat of hydration of hydraulic cementitious materials using Isothermal Conduction Calorimetry) using an isothermal calorimeter (Figure 3.15). A 100-gm mortar sample extracted from concrete using a #4 sieve was used for the test. The test was run for 72 hours after the mix and the generation of heat was reported with time.

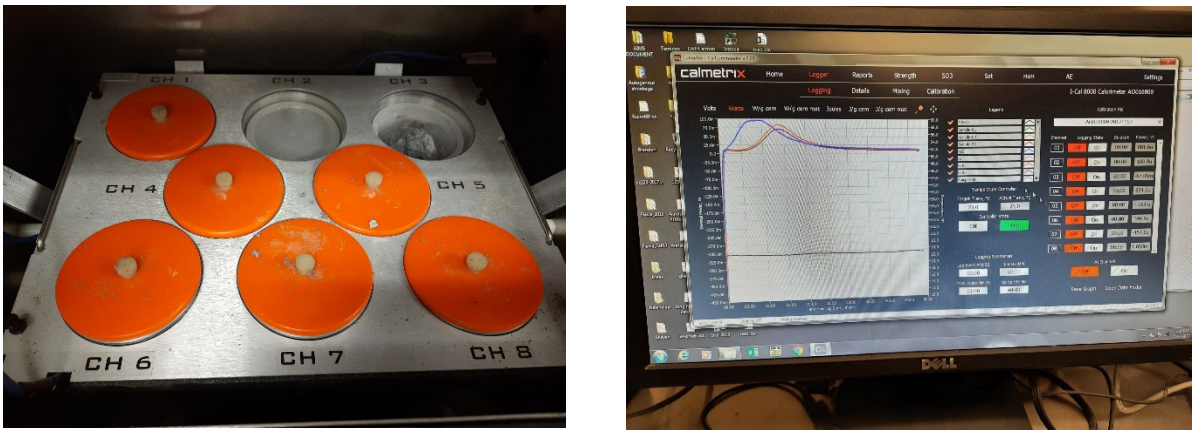

Figure 3.15 Chamber of isothermal calorimeter (left), and plot of recorded data in an associated computer (right)

3.7 Specimen Casting and Curing

The number of specimens cast and tested per batch for mechanical and durability properties is presented in Table 3.6.

Table 3.9 Number of Specimens

Test	Specimen Type	Count	Test Age	Curing Time
Compressive strength	4”X8” cylinder	3	7-days	7-days
		3	28-days	28-days
4-point bending	6”X6”X20” prism	3	28-days	28-days
Modulus of elasticity	4”X8” cylinder	3	28-days	28-days
Push-off testing	-	2	14-days	14-days
Pull-out of bars	-	6	14-days	14-days
Slant shear	Casted on diagonally half-cut 4”X8” cylinder	3	28-days	28-days
Freeze-thaw cycling	3”X4”X16” prism	3	After every 30-cycles, total 300-cycles	14-days
Electrical resistivity	4”X8” cylinder	3	4, 7, 14, 28, 56, 84, 112-days	28-days
Rapid chloride penetration test	2” thick sample saw cut from 4”X8” cylinder	1	28-days	28-days
		1	84-days	28-days
Restrained shrinkage	1.5” thick, 6” height, and 13” inside diameter ring	2	28-days or till crack, whichever is lower	1-day
Free shrinkage	3”X3”X11.25” prism	4	14, 18, 25, 32, 46, 74, 102, 130-days	14-days

All the specimens were cast according to ASTM C192 (Standard Practice for Making and Curing Test Specimens in the Laboratory). Samples were demolded after 24 hours, except those with long set times were demolded after 36 hours. After demolding, all the samples were stored in a curing chamber at 73.5 ± 3.5 ^{o}F (23.0 ± 2.0 ^{o}C) temperature and 100% R.H. till the test date.

3.8 Mechanical Properties

3.8.1 Compressive Strength

The compressive strength test was performed according to ASTM C39 (Standard Test Method for Compressive Strength of Cylindrical Concrete Specimens) with an end-grinded 4" by 8" cylinder (Figure 3.16). An average of three tests were reported for the 28-day compressive strength.

Figure 3.16 Compressive strength test setup

3.8.2 Modulus of Rupture

The modulus of rupture of concrete was tested using a simple beam with 4-point loading (Figure 3.17) according to ASTM C78 (Standard Test Method for Flexural Strength of Concrete). Three specimens of 6" by 6" by 20" (150 mm by 150 mm by 500 mm) were tested in air-dry conditions after 28 days of curing and the average was reported.

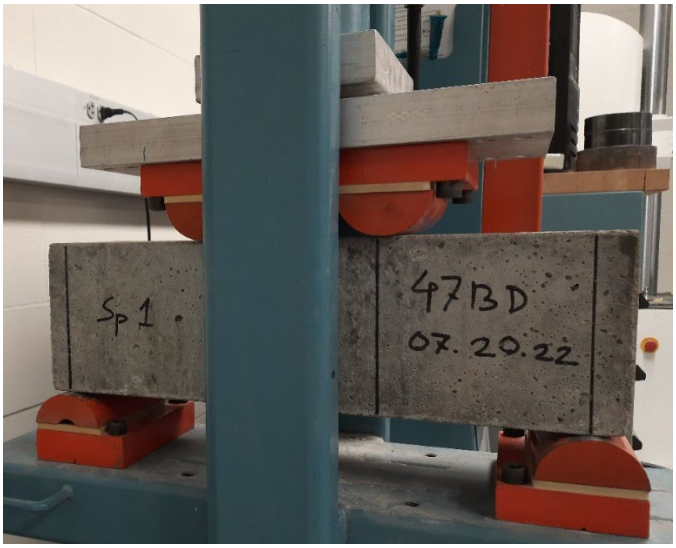

Figure 3.17 4-point bending flexural test setup

3.8.3 Static Modulus of Elasticity

The static modulus of elasticity (MOE) was tested according to ASTM C469 (Standard Test Method for Static Modulus of Elasticity and Poisson's Ratio of Concrete in Compression) to evaluate the stiffness of concrete. Three 4" by 8" cylinders were tested after 28 days of curing and the average value was reported. Deformation was measured in a gauge attached to the test setup shown in Figure 3.18. The MOE test setup is designed in a way that point c is fixed with a pivot rod, b is the center of the specimen, and the gauge is located at point a, as shown in Figure 3.19. To get the deformation of the specimen at point b, the displacement reading at point a is divided by 2.

Figure 3.18 Static modulus of elasticity test setup

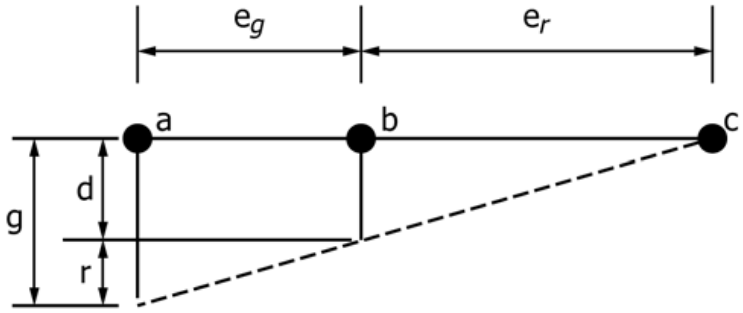

Figure 3.19 Displacement measurement diagram (ASTM C469)

Where,

d = displacement due to specimen deformation

r = displacement due to rotation of the yoke about the pivot rod

a = location of the gauge

b = support point of the rotating yoke

c = location of the pivot rod

g = gauge reading

3.8.4 Shear Strength

Push-off tests were conducted on two specimens for each mixture to evaluate the monolithic interface shear resistance according to Mattock and Hawkins (1972). Figure 3.20 shows the schematic view of the samples with dimension and the original formwork made for the sample. Figure 3.21 resembles the schematic and original view of the test setup. Each specimen had a shear plane that was approximately 11 in. deep and 5 in. wide. The specimens were designed to ensure that the failure of concrete occurs at the shear plane and undesirable failure modes due to bending or compression are avoided by providing sufficient steel on the other side of the sample. Samples were cast with ready-mix concrete. Forms were stripped after 24 hours and specimens were moist cured for 14 days. A push-off force was applied at a rate of 0.05 in./min and the vertical displacements across the shear plane were monitored using a string potentiometer. Average compressive strength ranged from 4.0 to 5 ksi at the time of testing.

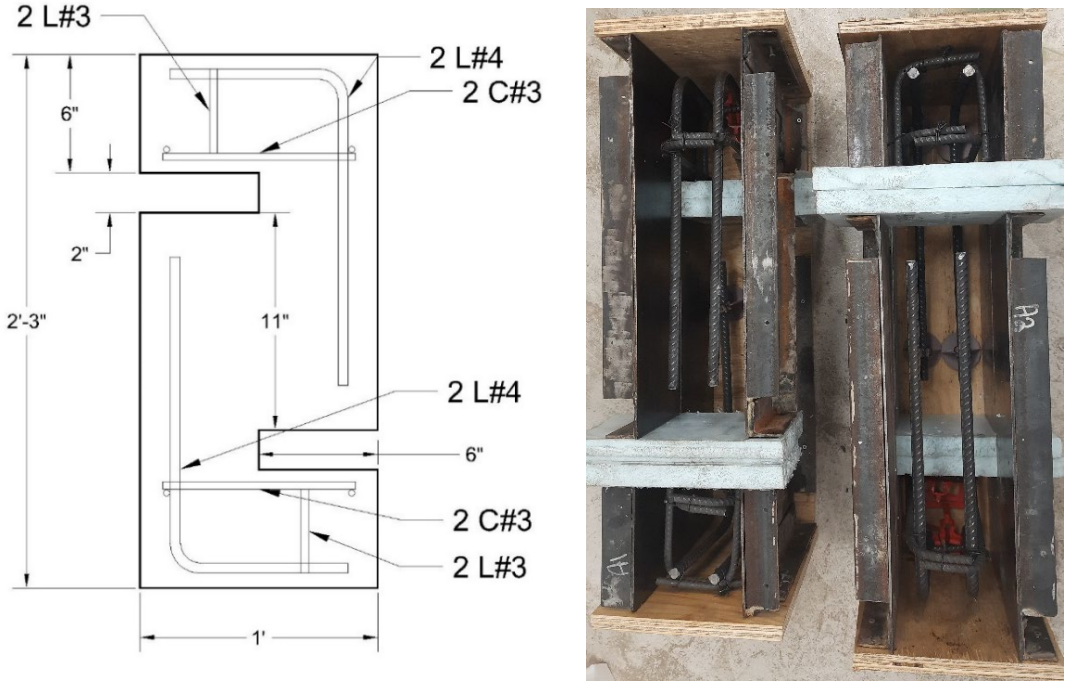

Figure 3.20 Schematic elevation view of the shear strength test specimen (left) and formwork (right)

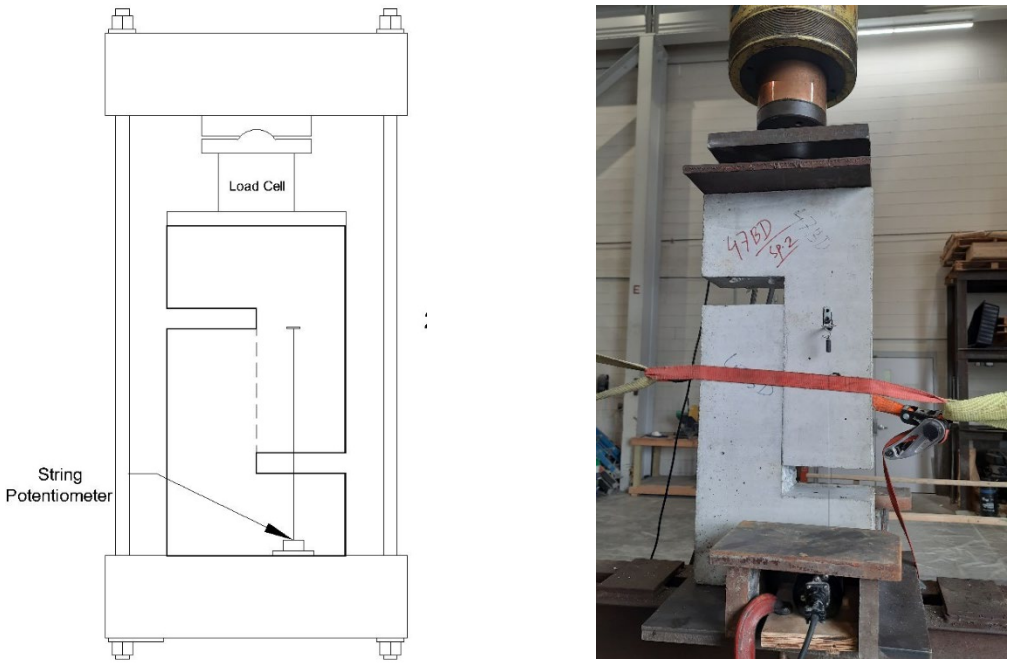

Figure 3.21 Shear strength test setup schematic view (left) and photo (right)

3.8.5 Bond Strength

Pull-out tests were conducted on two 4 ft x 2 ft x 0.67 ft rectangular concrete specimens (Figure 3.22). Since bar direction has a significant effect on the bond strength (CEB-fib, 2000), each specimen had three vertical and three horizontal bars to evaluate the bond strength. Epoxy-coated #5 Grade 60 deformed reinforced steel bars were tested for tension according to RILEM/CEB/FIP (1970). Horizontal bars typically used in bridge decks and vertical bars typically used in bridge rails were placed at 8” spacing in the center. The deboned length was ensured by attaching a plastic pipe to the top 4.875 in. of the bar resulting in a bonded length of 3.125 in. Forms were stripped after 24 hours, and the specimens were moist-cured for 14 days. A pull-out force was applied, and the ultimate load for the bond failure was measured using a load cell.

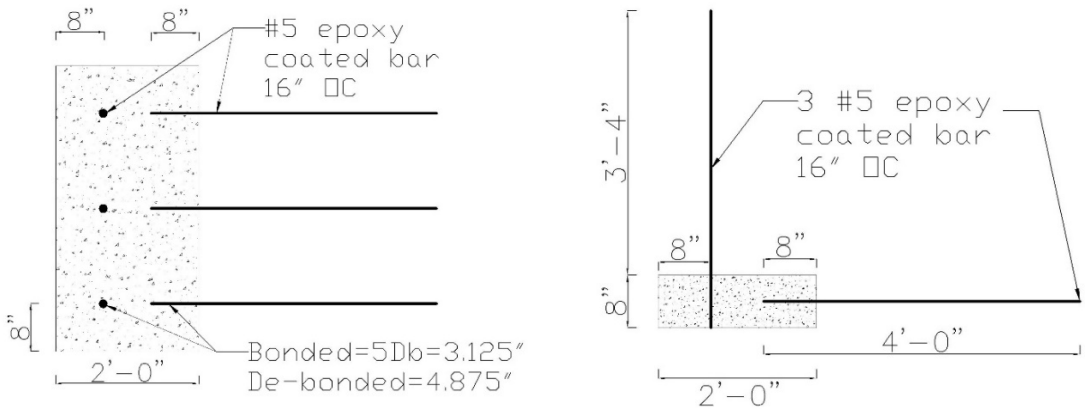

Figure 3.22 Bond strength test specimen schematic plan view (left) and elevation view (right)

3.8.6 Slant Shear Strength

The bond strength between fresh and hardened concrete was measured according to ASTM C882 (Standard Test Method for Bond Strength of Epoxy-Resin Systems used with Concrete by Slant Shear). However, instead of an epoxy-resin system, the concrete-concrete bond was tested. Dummy cylinder samples of 47BD (old concrete) were saw cut at a 30° vertical angle as shown in Figure 3.23 and grooved for bonding with new concrete. Each grooving was about 0.25 inches deep, 0.2 inches wide, and spaced 2 inches from each other. New concrete from each mix was then poured over the top of the pre-wetted grooved cylinder (47BD) as shown in Figure 3.24. The sample was demolded after a day or two and cured for 28 days. Three composite cylinders were compression tested according to ASTM C39 as presented in Figure 3.25. The bond strength was calculated by dividing the failure load by the bonding surface area and an average of three tests were performed for every mix. Failure of the bond is shown in Figure 3.26.

Figure 3.23 Prepared surface of old concrete (47BD)

Figure 3.24 Slant shear specimens after casting

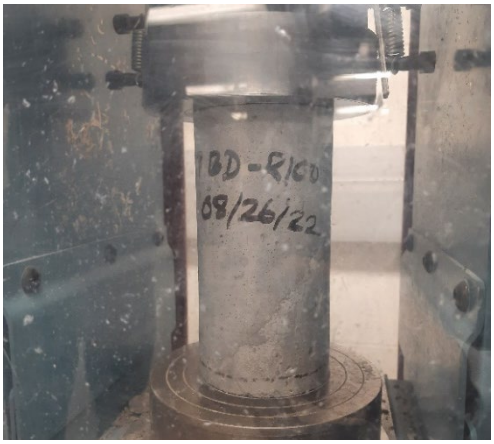

Figure 3.25 Slant shear test setup

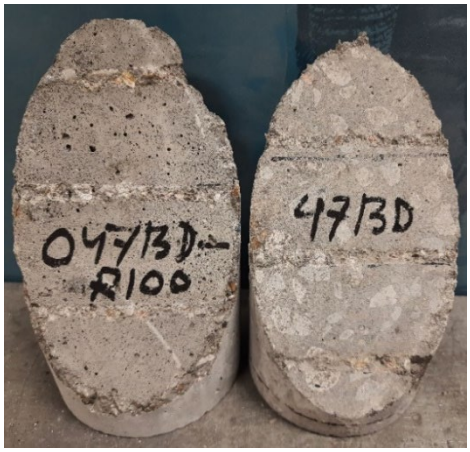

Figure 3.26 Failed surface after slant shear test

3.9 Durability Properties

3.9.1 Freeze-Thaw (F-T) Resistance

A freeze-thaw (F-T) resistance test was performed according to ASTM C666 (Standard Test Method for Resistance of Concrete to Rapid Freezing and Thawing) for procedure A. Three 3” by 4” by 16” prisms were cast per mixture and cured for 14 days before placing them in the F-T chamber. The Humboldt freeze-thaw cabinet with multiple channels (including one controlled) is shown in Figure 3.27 as the F-T chamber. Each sample was tested after every 30 cycles of freezing-thawing using a Sonometer (Resonance Frequency Test Apparatus) (Figure 3.28) for 300 cycles in total. Considering continuous freezing-thawing as a dynamic load on concrete, a relative dynamic modulus of elasticity (RDME) was reported with respect to every 30 cycles. The percentage of mass loss was also recorded to present the degradation of concrete with respect to time (F-T cycle). The degradation of concrete found in visual inspection during the test was also presented with a photo.

Figure 3.27 Concrete specimens in the freeze-thaw chamber

Figure 3.28 F-T resistance test setup with sonometer

3.9.2 Surface Resistivity

Surface resistivity was tested with a 4 in. x 8 in. cylinder following the AASHTO TP 95-14 guideline (Standard Method of Test for Surface Resistivity Indication of Concrete's Ability to Resist Chloride Ion Penetration). The peripheral surfaces (Figure 3.29) of three samples were tested in a saturated surface dry condition and the average was reported with standard deviation. The result was compared to Table 1 in AASHTO TP 95-14 to categorize the chloride ion penetrability of the mix.

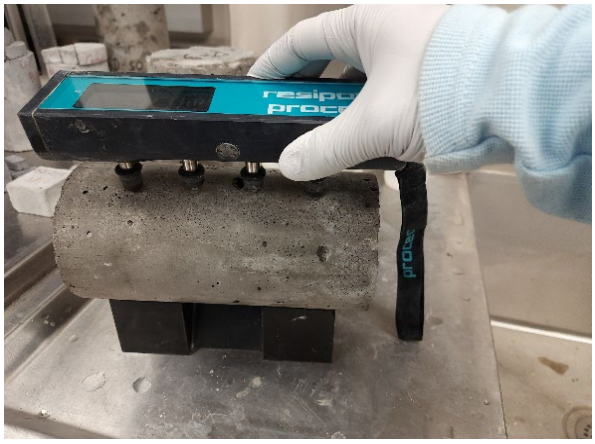

Figure 3.29 Surface resistivity test of concrete

3.9.3 Chloride Ion Penetrability

The penetrability of chloride ions in concrete was measured by the Rapid Chloride Penetration Test (RCPT) according to the ASTM C1202 (Standard Test Method for Electrical Indication of Concrete's Ability to Resist Chloride Ion Penetration) standard guideline. Initially one sample was tested per mixture for 28 days and 112 days, but later the sample count was raised to three-per-mix. ASTM C1202 suggests a longer curing period i.e., 112 days for the concrete containing SCM because the slow rate of its hydration decreases penetrability at a later age. Since the 1P cement used in this research already contains 25% SCM, a 112-day RCPT test was also performed. A 2±0.12 inches (50±3 mm) thick cylindrical concrete core sample (Figure 3.30) was saw cut from the top of a 4 in. x 8 in. cylinder. The two-inch circular perimeter of the sample was sealed with a protective solvent-free colored epoxy coating and later put into the vacuum chamber (Figure 3.31) for four hours. After a 16- to 20-hour break, the sample was placed in the Applied Voltage Cell (Figure 3.32) and the result was collected from the voltmeter after a six-hour run. The result was compared to table X1.1 in the appendix of ASTM C1202 to categorize the penetrability of the mix.

Figure 3.30 Saw-cut concrete specimen for rapid chloride penetration test

Figure 3.31 Sample preparation in vacuum saturation chamber

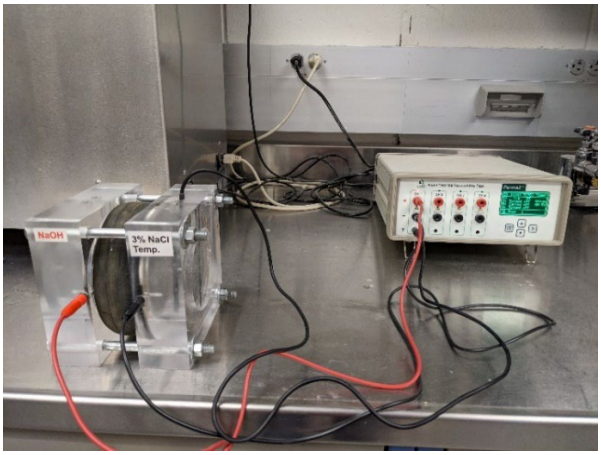

Figure 3.32 RCPT test in applied voltage cell

3.10 Shrinkage

3.10.1 Restrained Shrinkage

The restrained shrinkage sample was cast and tested following the standard ASTM C1581 (Standard Test Method for Determining Age at Cracking and Induced Tensile Stress Characteristics of Mortar and Concrete under Restrained Shrinkage). Two concrete samples were cast for each mixture. Figure 3.33 shows the standard mold of steel ring prepared for concrete casting. The outer ring attaching bolts were loosened after casting the sample to avoid any

external pressure. The concrete ring was cured with wet burlap for the first 24 hours and loss of moisture was prevented with wet burlap and plastic wrap. After 24 hours, the outer ring was taken out (Figure 3.34) and the concrete sample with an inner ring was placed in the environmental chamber at a controlled temperature of 73.5 ± 3.5 °F (23.0 ± 2.0 °C) and 50 ± 4.0% R.H. for 28 days or until concrete cracking indicated stress release. Strain gauges were attached inside of the inner ring to measure the stress generated from concrete shrinkage and recorded every two minutes with the datalogger (NI 9235). The reading was monitored for 28 days unless cracks happen earlier. A sudden decrease of strain reading of more than 30 micro strain is usually considered cracking. Concrete crack ages were reported to the nearest 0.25 days.

Figure 3.33 Restrained shrinkage test standard steel mold

Figure 3.34 Concrete test specimen in the environmental chamber

3.10.2 Free Shrinkage

Four concrete prisms (3” x 3” x 11.25”) were cast for the free shrinkage test according to ASTM C157 (Standard Test Method for Length Change of Hardened Hydraulic-Cement Mortar and Concrete). The concrete prisms were demolded after 24 ± 0.5 hours of casting and put in the curing room for another 13 days. After that, the initial comparator reading was taken as shown in Figure 3.35 and then specimens were transferred to the environmental chamber with a controlled temperature of 73.5 ± 3.5 °F (23.0 ± 2.0 °C) and 50 ± 4.0% R.H. for three more months. The

change of specimen length was recorded at shrinkage ages of 4, 7, 14, 28, 56, 84, and 112 days, which corresponds to 18, 21, 28, 42, 70, 98, and 126 specimen age in days, respectively.

Figure 3.35 Change of concrete length measurement

Chapter 4 Experimental Investigation

4.1 General

The main objective of this chapter is to present the experimental investigations conducted in Phase 1 (Preliminary Investigation) and Phase 2 (Comprehensive Investigation). The aggregate particle packing method, Modified Toufar Model, reported by Mamirov et al. (2021) was used to optimize the gradation of the locally available aggregate in Nebraska for bridge deck and rail concrete mixtures. Details of aggregate properties and the gradation optimization process were discussed in Chapter 3. The effects of gradual reduction of cementitious material content by 50 lbs., 100 lbs., and 150 lbs. per cubic yard of concrete are presented and discussed in this chapter. Findings of the experimental investigation are discussed, and conclusions and recommendations are made.

4.2 Preliminary Investigation

The feasibility of the RCMC was investigated by making small batches 1.2 to 1.5 ft^3. Fresh properties of concrete were monitored along with compressive strength and chloride ion penetration to ensure the workability, strength, and durability of new mixes.

4.2.1 Preliminary Mix Proportions

Mix 47BD, a typical bridge deck concrete mix in Nebraska, was used as a reference mix throughout this study. Adjustment in the quantity of materials for all other mixes was done from the standard required quantities of this 47BD mix for comparison. Besides the reference and optimized mix (O47BD), additional mixes were evaluated to better understand the effect of cementitious materials content reduction. With optimized gradation of aggregates, cementitious materials content gradually decreased by 50 lbs. (O47BD-R50), 100 lbs. (O47BD-R100), and 150 lbs. (O47BD-R150). The mix proportions that only passed the standard workability, strength, and electrical resistivity requirements for bridge deck concrete are presented in Table

4.1. Mix identifications are named according to the amount of cementitious materials content reduction (in pound unit) and aggregate gradation optimization. For example, O47BD-R150 denotes the concrete mix where the optimum aggregate blend was used in the 47BD mix with 150 lbs. reduction of cementitious materials per cubic yard (cy) of concrete (Figure 4.1).

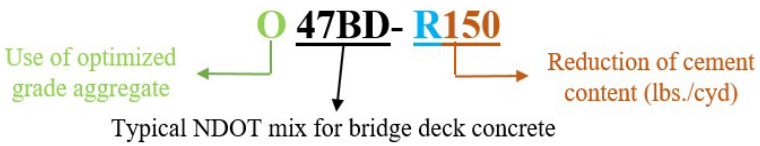

Figure 4.1 Mix identification

Table 4.10 Preliminary mix proportions

Mix ID	Cementitious Materials (lb/cy)	Water (lb/cy)	Limestone (lb/cy)	Sand & Gravel (lb/cy)	WR (fl oz/cwt)	AEA (fl oz/cwt)
47BD	658	263	862	1965	8.0	1.5
47BD-R100	558	222	930	2124	8.0	1.2
O47BD	658	263	1293	1543	8.0	1.3
O47BD-R50	608	249	1354	1630	16.0	1.5
O47BD-R100	558	229	1398	1683	18.0	1.2
O47BD-R150	508	208	1443	1738	24.0	0.5

N.B.: w/cm ratio was maintained at 0.41
WR: Water Reducer
AEA: Air-Entraining Agent

The 0.41 water-cementitious materials ratio was maintained in all mixes. The proportion of aggregate in 47BD and 47BD-R100 mix was 70% sand and gravel (SG), and 30% limestone (LS). In all other optimized mixes, a ratio of 55% SG and 45% LS was used instead. With the reduction of cementitious materials paste in concrete, more water-reducing admixture was needed to maintain the standard slump and flow of concrete. The use of optimized grade aggregate helps to reduce the excess void content expected for the reduction of cementitious materials paste from concrete. On the other hand, high dosages of water-reducer (WR) partially

help to generate some entrained air. All of this reduces the need for an air-entering admixture (AEA) in RCMC concrete.

4.2.2 Fresh Concrete Properties

Cementitious materials paste plays a vital role in concrete flow. It was important to ensure adequate concrete flow after the reduction of cementitious materials content. The vibrating L-box test was performed to check and compare concrete flow with the existing mix. The slump test evaluated the consistency of the concrete mixtures. With a less cementitious materials paste, more air void generates in the concrete. Therefore, unit weight and air content were measured to guarantee the density and air in the concrete to ensure the durability of the new mix.

Table 4.11 Fresh concrete properties

Mix ID	Slump (in)	Unit weight (lb)	Air content (%)	Workability under vibration		
				T_4^* (sec.)	T_6^* (sec.)	D_f^* (in.)
47BD	5.00	141.00	7.0	1.75	2.50	9.50
47BR-R100	1.50	-	-	2.00	-	5.50
O47BD	5.00	143.36	7.2	1.00	1.50	10.50
O47BD-R50	4.75	142.20	8.5	1.50	2.50	9.50
O47BD-R100	4.25	142.40	8.2	2.00	2.50	8.50
O47BD-R150	4.50	143.52	8.0	1.50	2.25	8.50
Targeted / Range	4.00 – 6.00	Comparison Only	6.0 – 8.5	Comparison Only	Comparison Only	Comparison Only
Standard / Source	ASTM C143 (AASHTO T119)	ASTM C138 (AASHTO T121)	ASTM C231 (AASHTO T152)	Nevada DOT (Report No. 366-16-803)		

*Note: T_4 - Flow time of concrete to reach 4-in mark under vibration in vibrating L-box test
T_6 - Flow time of concrete to reach 6-in mark under vibration in vibrating L-box test
D_f - Final flow distance of concrete under vibration in vibrating L-box test

Table 4.2 shows that the slump and air content of all mixes are acceptable. A gradual increase of unit weight during cementitious materials reduction denotes the benefit of aggregate packing optimization and the densification of reduced cementitious materials concrete. Hu and Wang (2005) showed that aggregate size and gradation have significant impact on concrete flow

when the sand-to-cement ratio is higher (s/c=3). All the mixes in this study have an s/c ratio of three or above. Smith and Collis (2001) also proved that optimized grade aggregate (or well-packed aggregate) has less void between particles than poorly-graded aggregate and requires less cementitious materials paste to fill the void. Thus, the additional cementitious materials paste coats the aggregate particles and improves the concrete flow. In the 47BD-R100 mix, the concrete flowed 5.5 inches, dramatically lower than the reference mix (47BD) flow of 9.5 inches as the aggregate gradation is not optimized and cementitious materials content was decreased by 100 lbs. On the other hand, even after reducing 150 lbs. of cementitious materials in combination with the optimized pack aggregate (O47BD-R150) the concrete flowed 8.5 inches in 5 seconds in the vibrating L-box test, which is comparable with the 9.5-inch flow of the reference mix.

4.2.3 Compressive Strength

Compressive strength was tested according to ASTM C39 & AASHTO T 22 for three 4 in. x 8 in. cylinders after 7 days and 28 days of standard moist curing for each specimen. Figure 4.2 shows that all RCMC mixes passed the 28-day compressive strength NDOT requirements (4000 psi), marked with a dotted line in Figure 4.2. Since the cementitious materials content was reduced without any change in the water-cementitious materials ratio (0.41), the total amount of water in the concrete was 24% lower in the O47BR-R150 mix compared to the reference mix. The strength of O47BR-R50 and O47BR-R100 were very comparable to that of the reference mix. Standard deviation (SD) in the strength test data was not reported in Figure 4.2 since not enough data according to ACI 214R-11 was available at this stage.

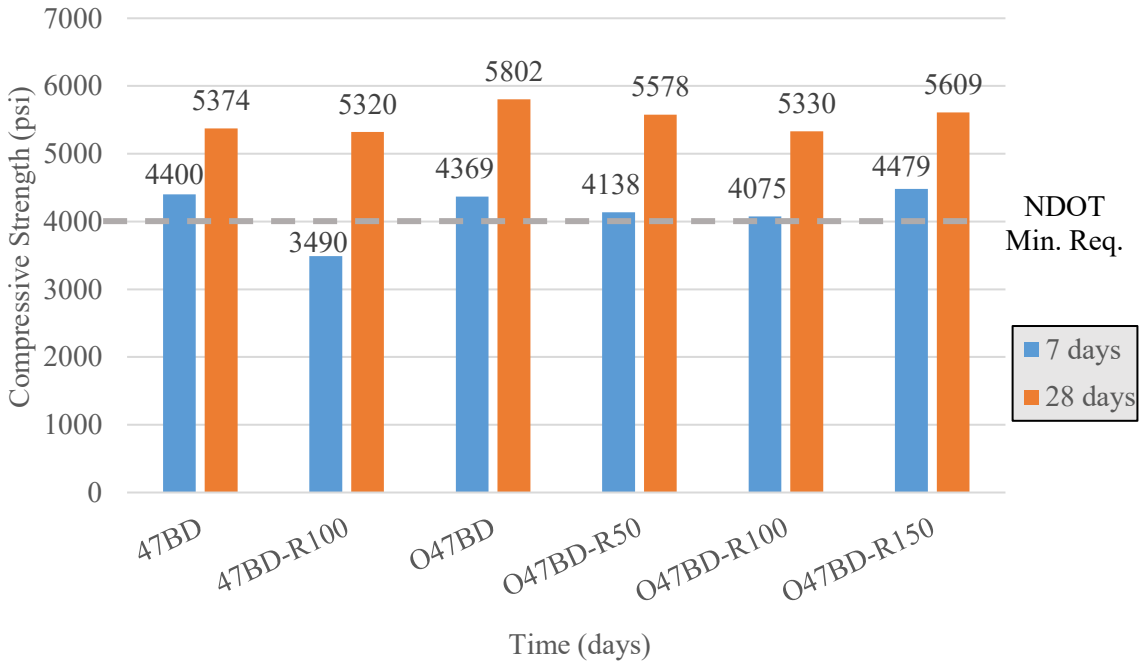

Figure 4.2 Comparison of compressive strength of preliminary mix

4.2.4 Surface Resistivity to Chloride Ion Penetration

The electrical resistivity (both surface and bulk resistivities measured according to AASHTO TP 95) of all concrete mixtures is shown in Figures 4.3 and 4.4. Table 4.3 presents the AASHTO TP95 chart for the standard electrical resistivity range of concrete. Along with the reference and three optimized mixes, two more mixes were performed for better understanding. One is the reference mix with optimized gradation and no cementitious materials reduction (O47BD) and the other is the reference mix with 100 lbs of cementitious materials reduction but no aggregate optimization (47BD-R100). Due to some instrumental issues in the bulk resistivity apparatus, some long-term bulk resistivity data was not captured.

Optimization of aggregate packing increases the concrete density from the reference mix as observed in O47BD (Table 4.2). Since cementitious materials paste is more porous than the aggregate, reducing cementitious materials content also helps to increase concrete density (highest density recorded for O47BD-R150 concrete in Table 4.2) and is more resistive to

chloride ion penetration. Figures 4.3 and 4.4 also indicate that as the cementitious materials content decreases, the concrete resistivity increases, and the risk of corrosion with time decreases compared to the reference mix.

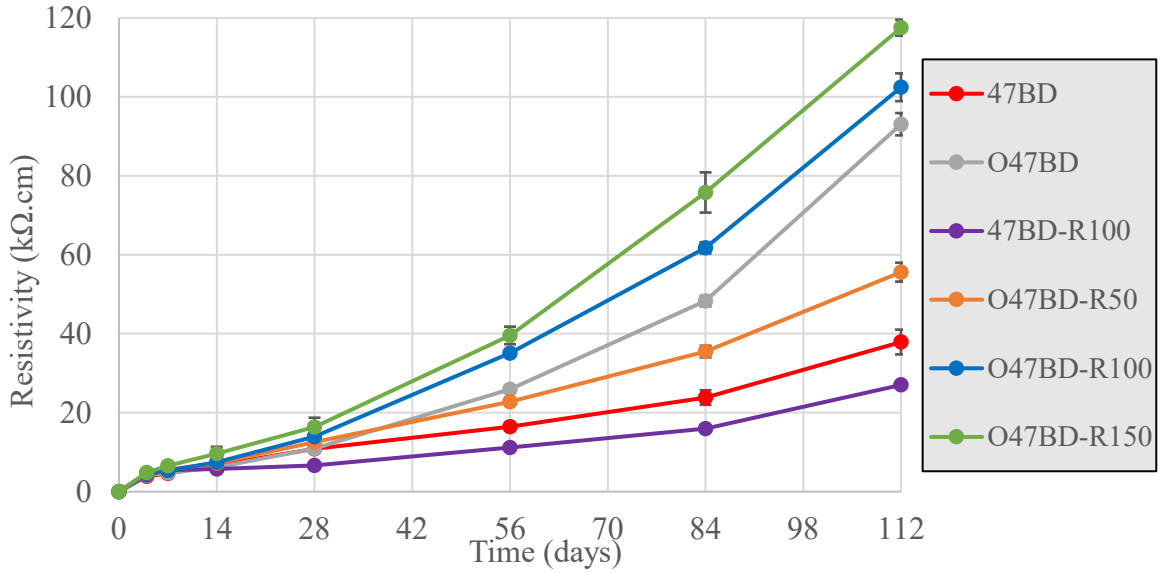

Figure 4.3 Electrical resistivity (surface)

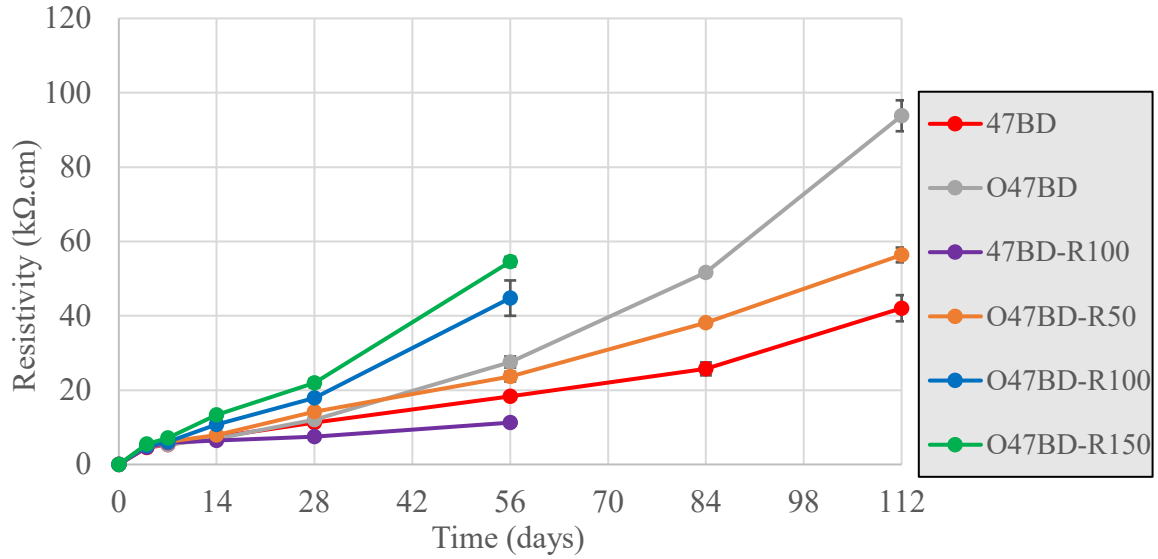

Figure 4.4 Electrical resistivity (bulk)

Table 4.12 Susceptibility of chloride ion penetration (AASHTO TP 95)

Surface Resistivity (kΩ-cm)	Chloride Ion Penetration
<12	High
12-21	Moderate
21-37	Low
37-254	Very Low
>254	Negligible

4.2.5 Preliminary Investigation Summery

Results of the preliminary investigation have shown that RCMC mixes with 50-, 100-, and 150-lbs cementitious materials reduction to satisfy the NDOT minimum requirements for bridge deck/rail concrete with respect to workability, strength, and chloride penetration. These tests and additional tests were conducted in Phase 2, which was the comprehensive experimental investigation.

4.3 Comprehensive Investigation

The scope of this investigation was to evaluate the properties of proposed mixtures with aggregate optimization and cementitious materials reduction. All the relevant fresh, early-stage, and hardened properties were tested and compared to the reference mixture.

4.3.1 Mix Proportions

Aggregate proportions of all mixes are presented in Table 4.4. The admixtures were adjusted based on the experience from the preliminary investigation. The water-cementitious materials ratio was controlled at 0.41 for all mixes to ensure consistency. Using a higher amount of LS, which is more angular than SG, helped to optimize aggregate gradation and reduce the demand for cementitious materials. Since the w/cm ratio was fixed, the lesser amount of cementitious materials required less water and a higher dosage of WR admixture to maintain the

workability. Also, dosage of AEA had to be reduced with the increase of WR to maintain the entrained air content within the acceptable range.

Table 4.13 Mix proportions for performance evaluation

Mix ID	Cementitious Materials (pcy)	Water (pcy)	Limestone (LS) (pcy)	Sand & Gravel (SG) (pcy)	WR (fl oz/cwt)	AEA (fl oz/cwt)
47BD	658	268	862	1965	10	1.5
O47BD-R50	608	249	1354	1630	18	1.3
O47BD-R100	558	229	1398	1683	21.8	1.2
O47BD-R150	508	208	1443	1738	29.2	1.0

N.B. – w/cm ratio was maintained as 0.41

4.3.2 Fresh Concrete Properties

Fresh concrete properties of all mixes are tabulated in Table 4.5 to compare the optimized and controlled mix performance. NDOT Standard Specifications for bridge deck concrete construction (2017) required 6.0 - 8.5% air content in the fresh concrete for durability reasons. All the mixes contained air in that range. Since the aggregate optimization reduced the void content, the unit weight of optimized mixes is larger than the reference mix. To ensure adequate workability of concrete, the usual practice in industry is to maintain the slump in a range of 4.0 - 6.5 in. Optimized mixes had lower slump than the control mix. The WR dosages had to be doubled for mixes with 50- and 100-lbs cementitious materials reduction and tripled for the mixture with 150-lbs cementitious materials reduction. The flow of concrete was also reduced with the reduction of cementitious materials content but still very comparable with the existing 47BD mix. Even after reducing 150 lbs of cementitious materials, it only took the O47BD-R150 mix 2.25 seconds to pass the 6-inch mark in the vibrating L-box test, which is 0.25 seconds longer than the time it took the 47BD mix. Results in this fresh stage show that it is feasible to

obtain an optimized mix with 150 lbs (1.5 sacks) of cementitious materials reduction per cubic yard of concrete.

Table 4.14 Fresh concrete properties for performance evaluation

Mix ID		47BD	O47BD-R50	O47BD-R100	O47BD-R150
Air Content (%)		8.50	7.00	7.50	8.00
Unit weight (lb/ft^3)		137.70	143.30	143.10	142.08
Slump (inch)		6.00	3.50	4.25	3.25
Flow under vibration	T_4^* (sec.)	1.50	2.00	2.00	1.50
	T_6^* (sec.)	2.00	2.50	2.50	2.25
	D_f^* (inch)	9.50	7.75	7.50	8.00

*T_4 = Flow time of concrete to reach 4-in mark under vibration
T_6 = Flow time of concrete to reach 6-in mark under vibration
D_f = Final flow distance

4.3.3 Early-Age Properties

Figure 4.5 and Table 4.6 show the initial and final set time of all mixes as measured using the penetration resistance data. These results indicate the significant increase in the initial and final set times for O47BD-R100 and O47BD-R150 mixes due to the increased use of WR admixtures. The 19 hours and 45 minutes recorded as the final set time for the O47BD-R150 mix is more than double the set time for the 47BD mix. This longer set time could make the mix unfeasible for bridge deck/rail construction. Additional chemical admixtures can be used to reduce the set time if needed.

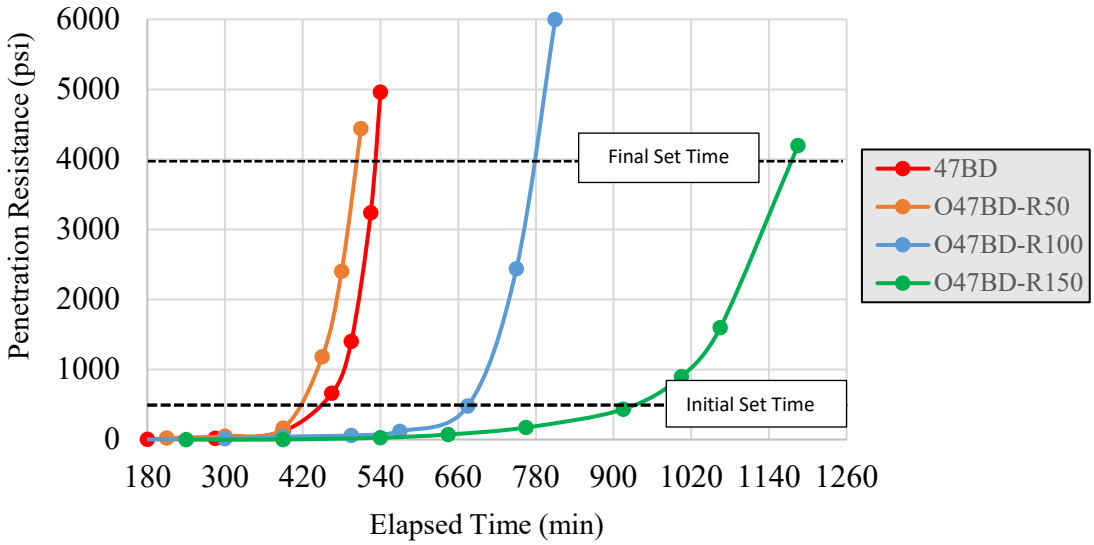

Figure 4.5 Initial and final set times of all mixes

Table 4.15 Set time of all mixes.

Mix ID	Initial Set Time	Final Set Time
47BD	7 hour 30 minutes	8 hour 55 minutes
O47BD-R50	7 hours	8 hour 25 minutes
O47BD-R100	11 hour 15 minutes	13 hours
O47BD-R150	15 hour 50 minutes	19 hour 45 minutes

Reduction of cementitious materials content decreases the amount of heat generation in the hydration reaction. Figure 4.6 shows that the change in heat of hydration is not noticeable in mixes with 50 lbs and 100-lbs cementitious material reduction; it is clearly noticeable in the mix with 150-lbs cementitious material reduction. A peak power was recorded for each optimized mix at times that mimic the order in which the mixes reached their setting times.

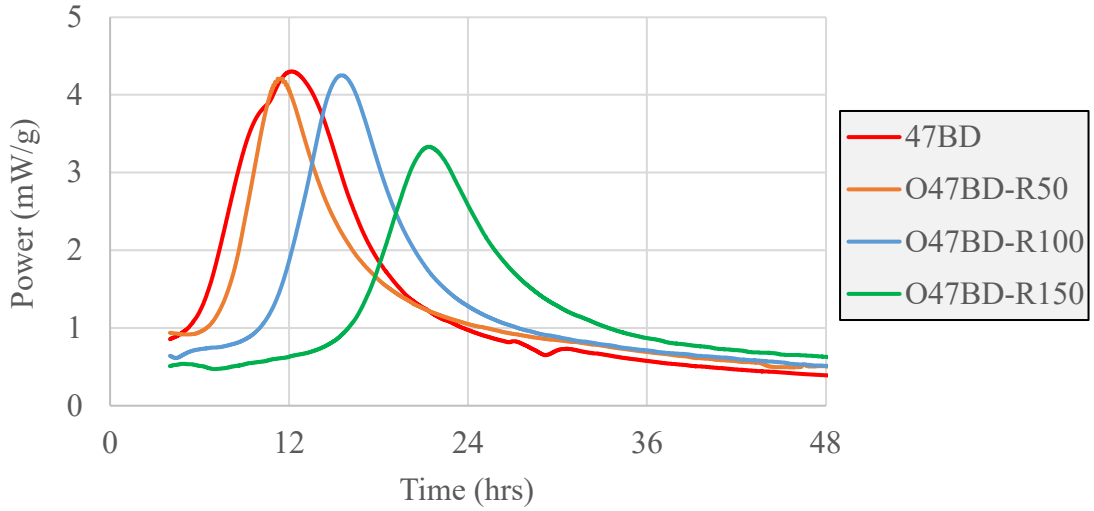

Figure 4.6 Heat of hydration of all mixes

4.3.4 Mechanical Properties

Figure 4.7 shows the compressive strength of all mixes at 7 and 28 days. All mixes passed the 28-day NDOT minimum strength requirement, which is 4000 psi. It is noticeable that all optimized mixes had higher strengths than the reference mixes. The 28-day compressive strength of the O47BD-R50, O47BD-R100, and O47BD-R150 mixes were 35%, 32%, and 28%, higher than that of the reference mix, respectively. This could be attributed to the increased use of LS with angular particles in optimized mixes making the concrete denser. With the decrease of cementitious material content from 50 to 150 lbs a slight gradual decrease in strength occurred. This could be an effect of the cementitious materials bond strength as there is less cementitious materials for the aggregate surface bond. In summary, reduction of cementitious materials content by optimizing aggregate gradation improves concrete strength even after a reduction of 150 lbs per cubic yard of concrete.

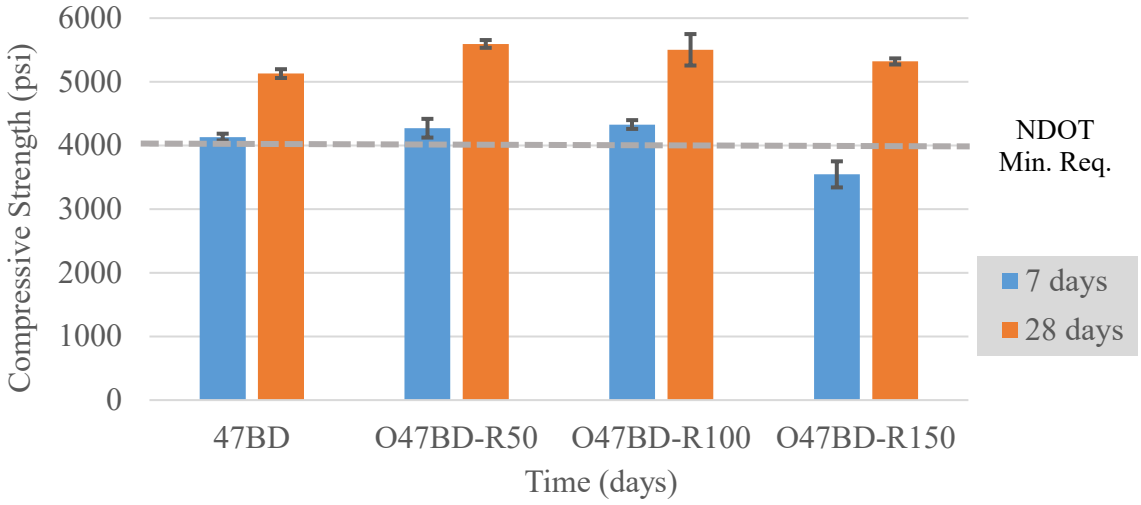

Figure 4.7 Compressive strength of all mixes

Figure 4.8 plots the modulus of rupture for the tested mixes. This figure indicates that there is no significant effect of cementitious materials reduction on the modulus of rupture of concrete.

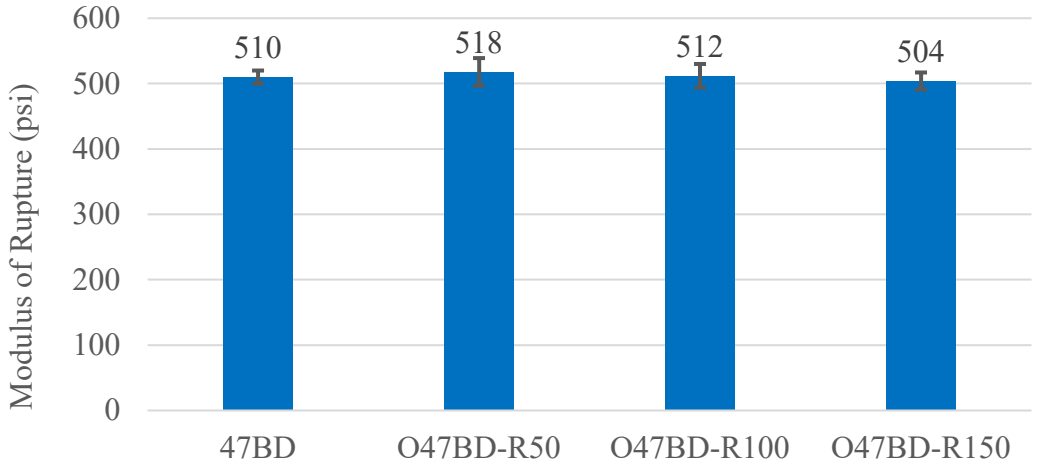

Figure 4.8 Modulus of rupture of all mixes

Figure 4.9 plots the measure modulus of elasticity (MOE) of all tested mixes. This figure indicates the MOE of optimized mixes is 2% to 11% higher than that of the control mix.

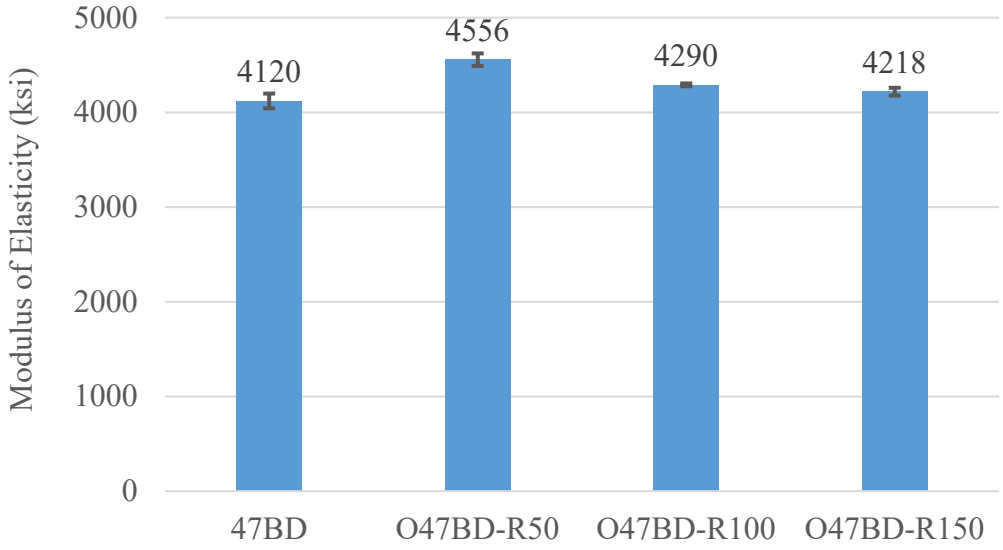

Figure 4.9 Modulus of elasticity of all mixes

The shear strength and concrete-rebar bond strength results are presented in the next chapter (Production Demonstration) as their specimens were cast using ready-mix concrete. The concrete-concrete bond strength was measured using the slant shear test. Figure 4.10 shows the test results, which indicate a significant bond increase of 72% and 11% for mixes with cementitious materials reduction of 50 lbs and 150 lbs respectively. As mentioned earlier, the angularity of LS particles and optimizing aggregate gradation help the bond with hardened concrete. However, continuous reduction of cementitious materials gradually decreases the bond strength as it did in other mechnical properties.

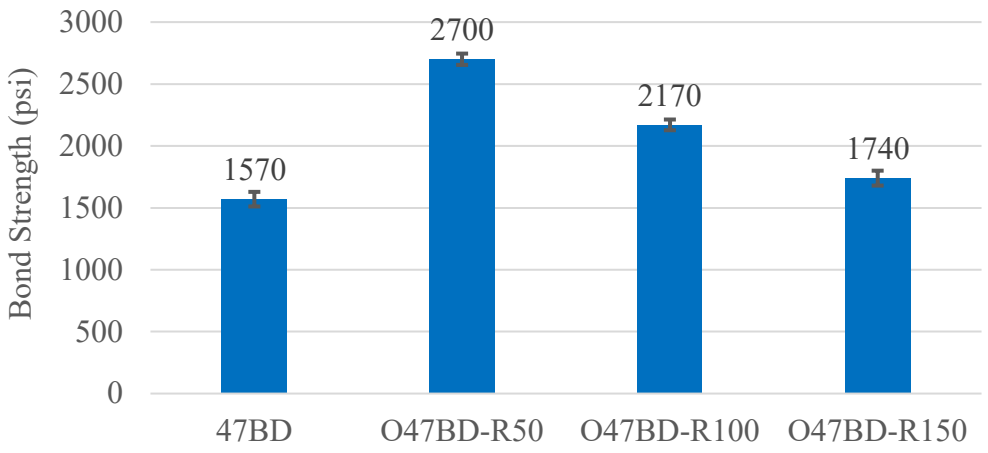

Figure 4.10 Concrete-to-concrete bond strength of all mixes

4.3.5 Durability Properties

Figure 4.11 demonstrates the relative dynamic modulus and Figure 4.12 demonstrates the mass change of the freeze/thaw (F/T) resistance test. The minimum requirements of NDOT are marked in yellow dash lines in these Figures. NDOT requires no less than 70% relative dynamic modulus and no greater than 5% mass change at 300 F/T cycles according to ASTM C666. As presented in Figures 4.11 and 4.12, all mixes pass these requirements. The O47BD-R100 mix has the least relative dynamic modulus and mass loss, while the reference mix, 47BD, had the highest relative dynamic modulus and mass loss at 300 cycles.

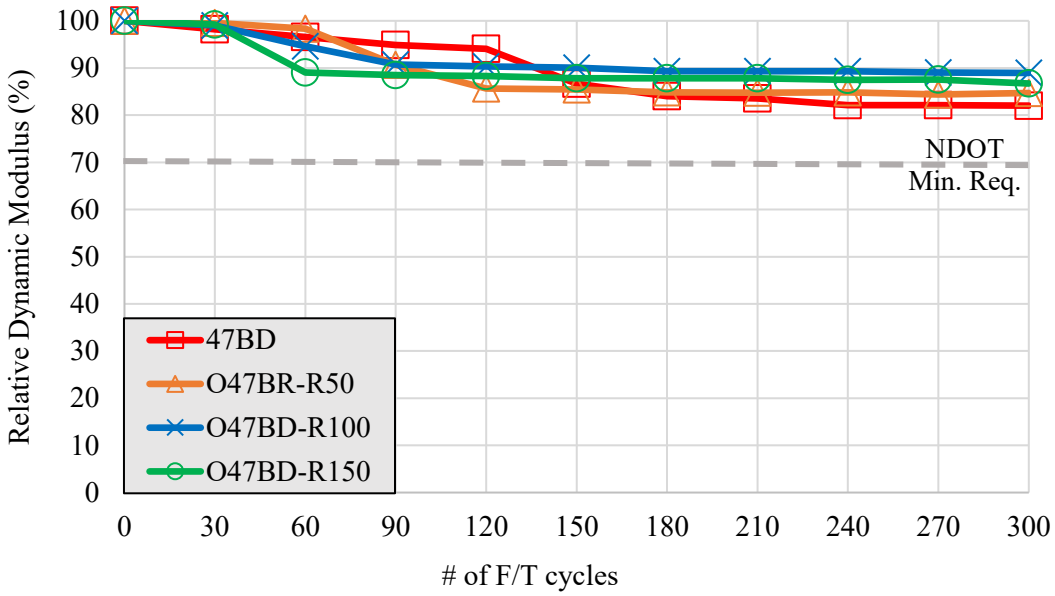

Figure 4.11 Mass change of all mixes in F-T resistance test

Figure 4.13 shows representative specimens for all mixes after 300 cycles of freezing and thawing. A close look at the pictures in the figure shows that the 47BD mix has degraded the most and the O47BD-R100 mix has degraded the least, which supports the experimental results.

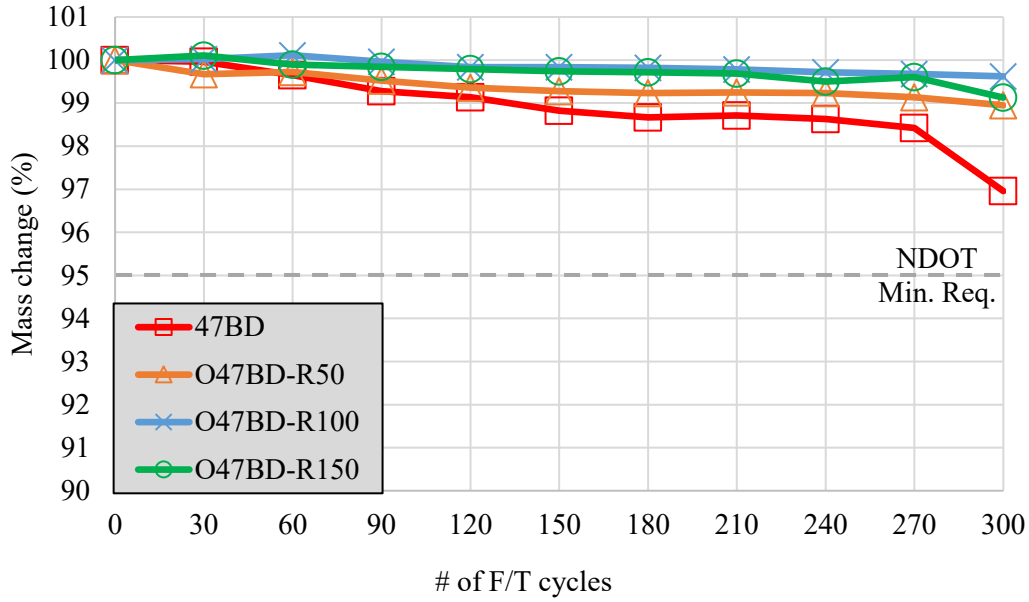

Figure 4.12 Relative dynamic modulus of all mixes

Mix ID	In 0 F/T cycle	After 300 F/T cycle
47BD	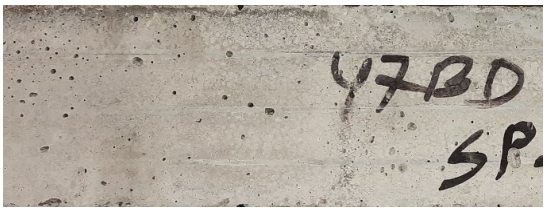	
O47BD-R50		
O47BD-R100		
O47BD-R150		

Figure 4.13 Representative specimens after 300 cycles of freezing-thawing test

The surface electrical resistivity is presented in Figure 4.14 for all mixes. The AASHTO TP95 standard for defining the resistivity level of concrete is presented in Table 4.7. Test results at 28 days indicate that all optimized mixes had a moderate level of chloride ion penetration, whereas the reference mix, 47BD, had a high level of chloride ion penetration. After 28 days, all mixes continued to have high electric resistivity, which means lower chloride ion penetration. Also, the higher the reduction of cementitious materials content, the higher the electric resistivity, which means lower chloride ion penetration.

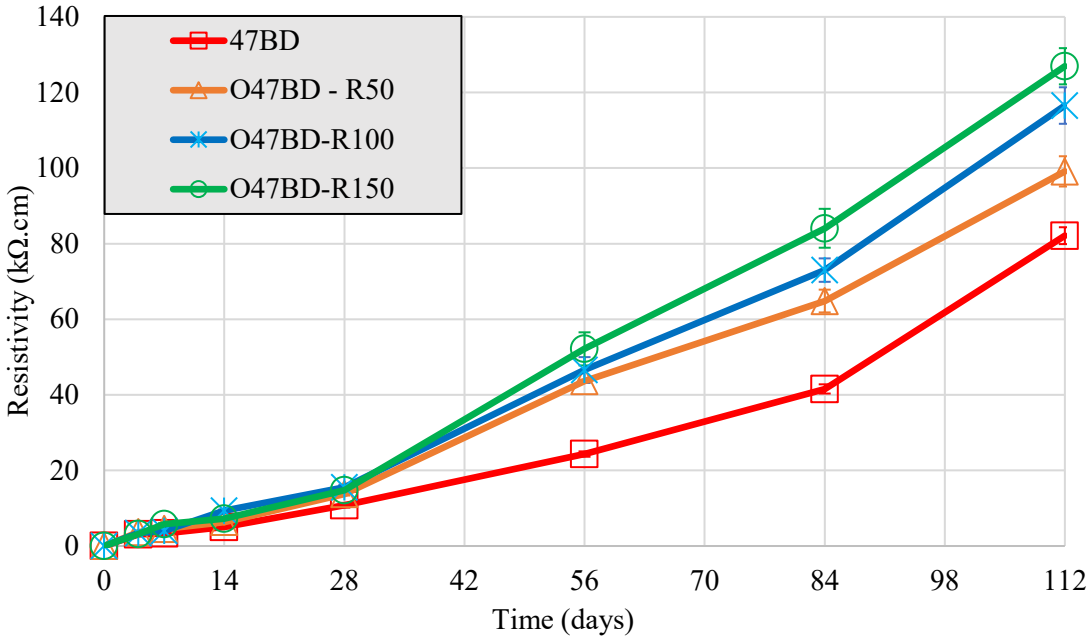

Figure 4.14 Electrical resistivity (surface) of all mixes

Table 4.16 AASHTO TP95 standard for electric resistivity

Electrical Resistivity (kΩ-cm)	Chloride Ion Penetration
<12	High
12-21	Moderate
21-37	Low
37-254	Very Low
>254	Negligible

The rapid chloride penetration test (RCPT) also supports the results obtained from the surface resistivity test. Figure 4.15 presents the RCPT results and Table 4.8 presents the chloride permeability classifications according to ASTM C1202. Test results indicate that the O47BD-R100 and O47BD-R150 mixes have very low permeability after 112 days whereas the O47BD-

R50 and 47BD mixes have low permeability. This also supports the conclusion that the higher the reduction of cementitious materials content, the lower the chloride ion permeability.

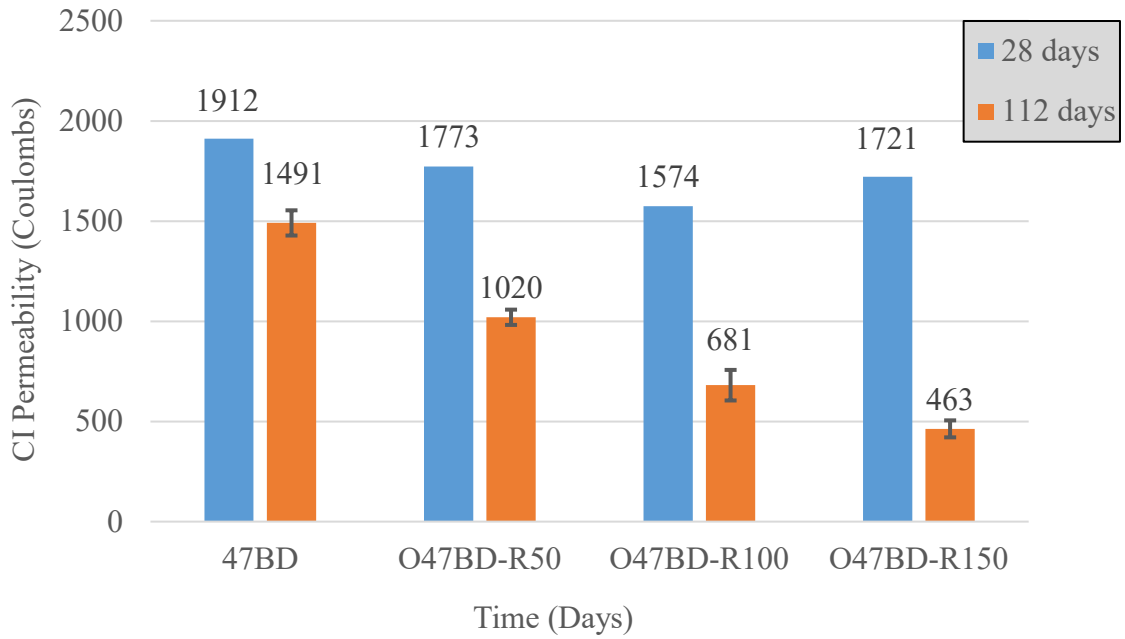

Figure 4.15 RCPT results for all mixes

Table 4.17 ASTM C1202 standard for chloride ion permeability

Charge Passed (Coulombs)	Chloride Ion Permeability
>4000	High
2000-4000	Moderate
1000-2000	Low
100-1000	Very Low
<100	Negligible

Figure 4.16 shows the free shrinkage test results of all mixes. As expected, the reference 47BD mix had the highest shrinkage strain due to the high volume of cementitious materials. All the optimized mixes had lower shrinkage strain than the reference mix, and the O47BD-R100

and O47BD-R150 mixes had almost the same shrinkage strain in the range of 400 – 500 micro-strain at 112 days.

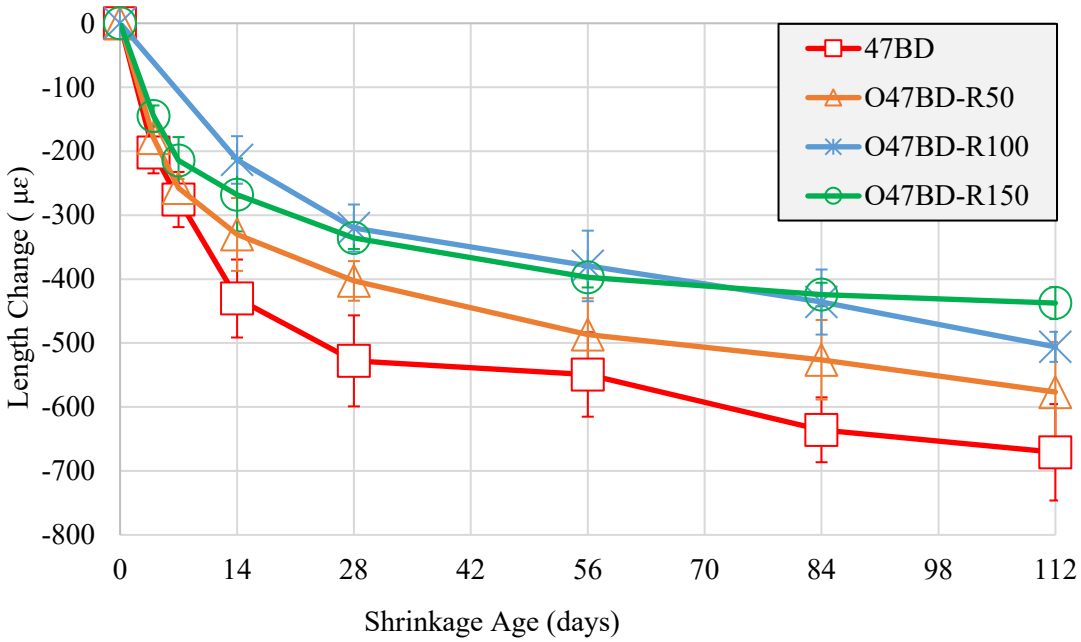

Figure 4.16 Free-shrinkage test results of all mixes

Figure 4.17 shows the restrained shrinkage test results for all mixes. As expected, the cracking time was delayed for the optimized mixes with reduced cementitious material content. The O47BD-R50 cracked after about 8 days, which is longer than the 5.25 days that was the cracking time for the reference 47BD mix. The reduction in cementitious materials content results in less paste and lower heat of hydration, which reduces shrinkage and makes the hardened concrete less prone to cracking. The O47BD-R100 and O47BD-R150 mixes cracked after 12 and 15.25 days, respectively. Figure 4.18 shows an example of cracking in a concrete specimen.

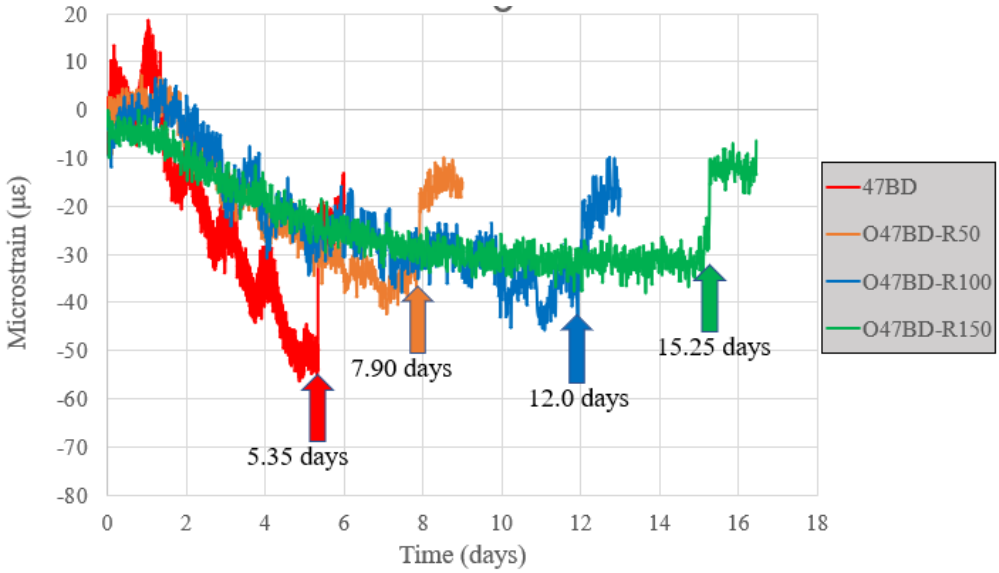

Figure 4.17 Restrained shrinkage test results of all mixes

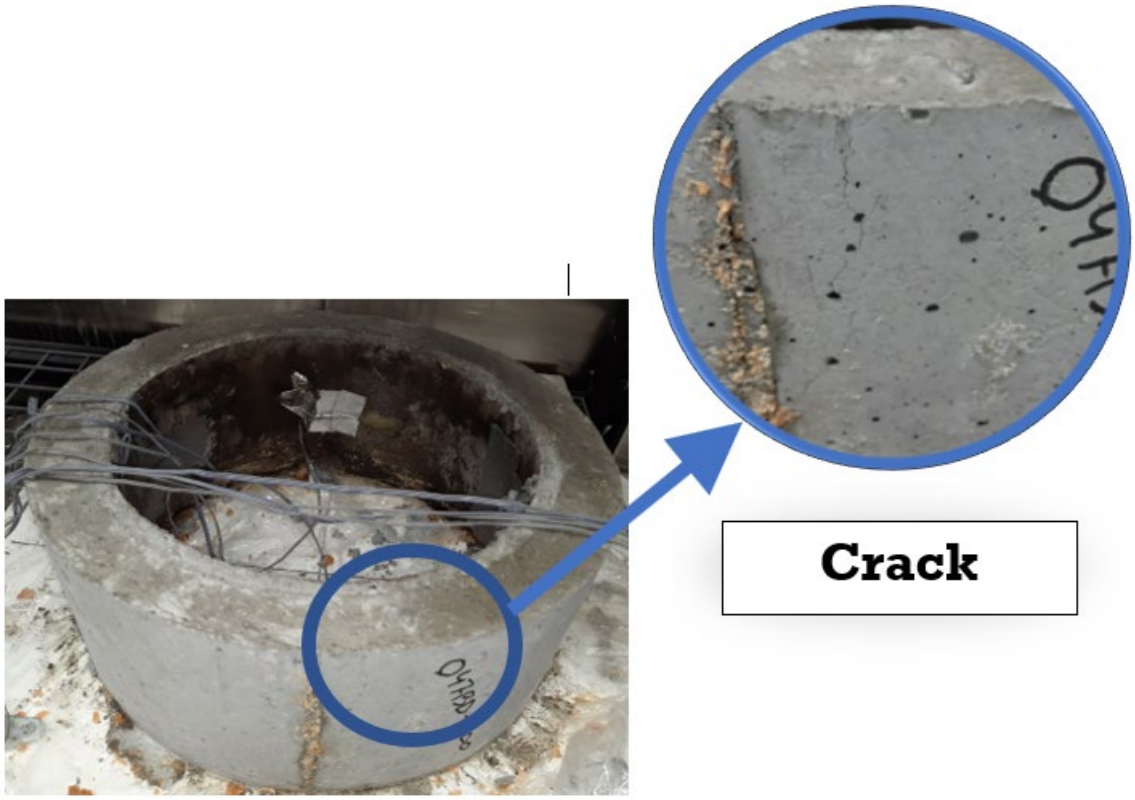

Figure 4.18 Restrained shrinkage crack in concrete

4.3.6 Summary of Comprehensive Investigation

Results of the comprehensive investigation have shown that all the RCMC mixes with 50-, 100-, and 150-lbs cementitious materials reduction satisfy the NDOT minimum requirements for bridge deck/rail concrete with respect to workability, strength, durability, and shrinkage. All the optimized mixes also performed better than the current 47BD mix except for O47BD-R150 that had very long final set time (19 hours 45 minutes).

Chapter 5 Production Mockup

5.1 General

This chapter presents the experimental work conducted to evaluate the feasibility of batching, mixing, transporting, pumping, and placement of reduced cementitious materials concrete (RCMC) mixes in a more realistic setting that simulates construction sites. Four deck slabs were cast using ready-mix concrete, one for each RCMC mix and the reference mix. These four slabs were then tested in a three-point bending test to compare their structural performance. The test results of concrete shear strength and concrete-rebar bond strength are also presented in this chapter. Restrained shrinkage samples were also taken and tested to verify the cracking time presented earlier.

5.2 Mix Design

The same mix proportions used in the comprehensive investigation presented in Chapter 4 were used to produce the mockup deck slabs. A ready-mix concrete quantity of four cubic yards was batched for mixtures 47BD and O47BD-R50, and five cubic yards for mixtures O47BD-R100 and O47BD-R150 because they were pumped. A summary of the batch tickets is presented in Table 5.1. The mid-range water-reducing admixture was used for the reference mix while the high-range water-reducing admixture was used for RCMC mixes to enhance their workability and pumpability.

Table 5.18 Summary of batch tickets

Mix ID (Date)	47BD (02/20/23)	O47BD-R50 (03/07/23)	O47BD-R100* (03/23/23)	O47BD-R150* (04/06/23)
47BFA (lb/cy)	2020	1615	1668	1723
47BCA (lb/cy)	880	1341	1385	1432
CEM-1PF (lb/cy)	658	608	558	508
MBPOLY1020 (oz/cwt)	6	-	-	-
MBGLEN3030 (oz/cwt)	-	4	5	5
MBAE90 (oz/cy)	8.75	4.25	4	5
WATER-LBS (lb/cy)	240	234	223	201
MBPOLY1020 MBGLEN3030 *	Mid-range water reducer High-range water reducer Concrete after pumping			

5.3 Mockup Specimen and Formwork

Concrete deck slab specimens were made using a job-built wooden form that was 10 ft long and 6.5 ft wide. The slab thickness of 7.5 inches was chosen as it is the minimum structural slab thickness for bridge decks according to NDOT bridge office policies and procedures. Figure 5.1 shows a schematic diagram of the deck slab form and reinforcement, while Figure 5.2 shows a photo of the completed form. Rebars were distributed in two layers: the top layer was made of #4 Grade 60 deformed bars at 12-inche spacing in both directions; and the bottom layer was made of #5 Grade 60 deformed bars at 12-inche spacing in both directions. The same form and reinforcement were used in fabricating all the four specimens.

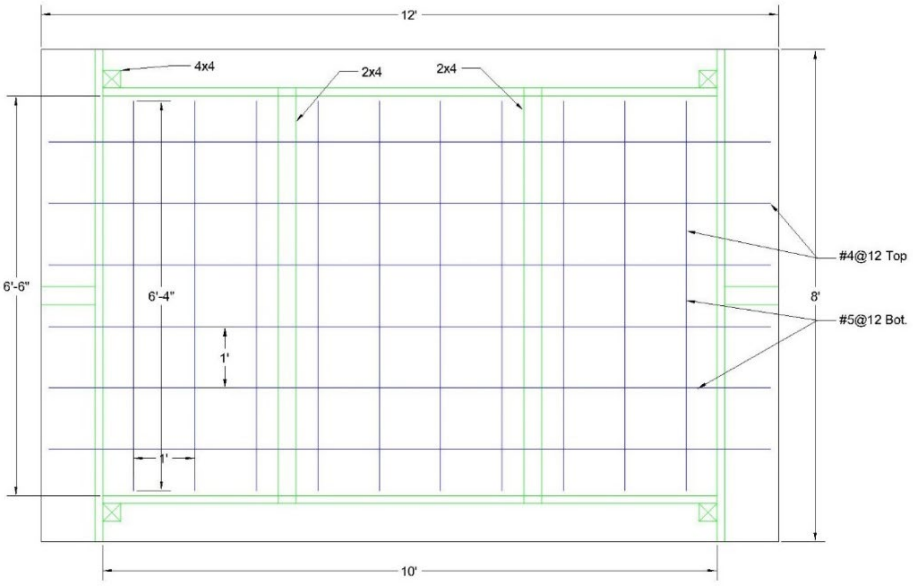

Figure 5.1 Dimensions and reinforcement of deck slab specimens

Figure 5.2 Form with rebars of deck slab specimen

5.4 Concrete Placing and Curing

For the 47BD and O47BD-R50 slab specimens, concrete was placed by the truck chute into the forms as shown in Figure 5.3 (a). For the O47BD-R100 and O47BD-R150 slab

specimens, concrete was placed by a concrete pump, a 100-ft-long pump boom, and hose as shown in Figures 5.3 (b) and (c) to evaluate the pumpability of these mixes when a significantly reduced cementitious material content is used.

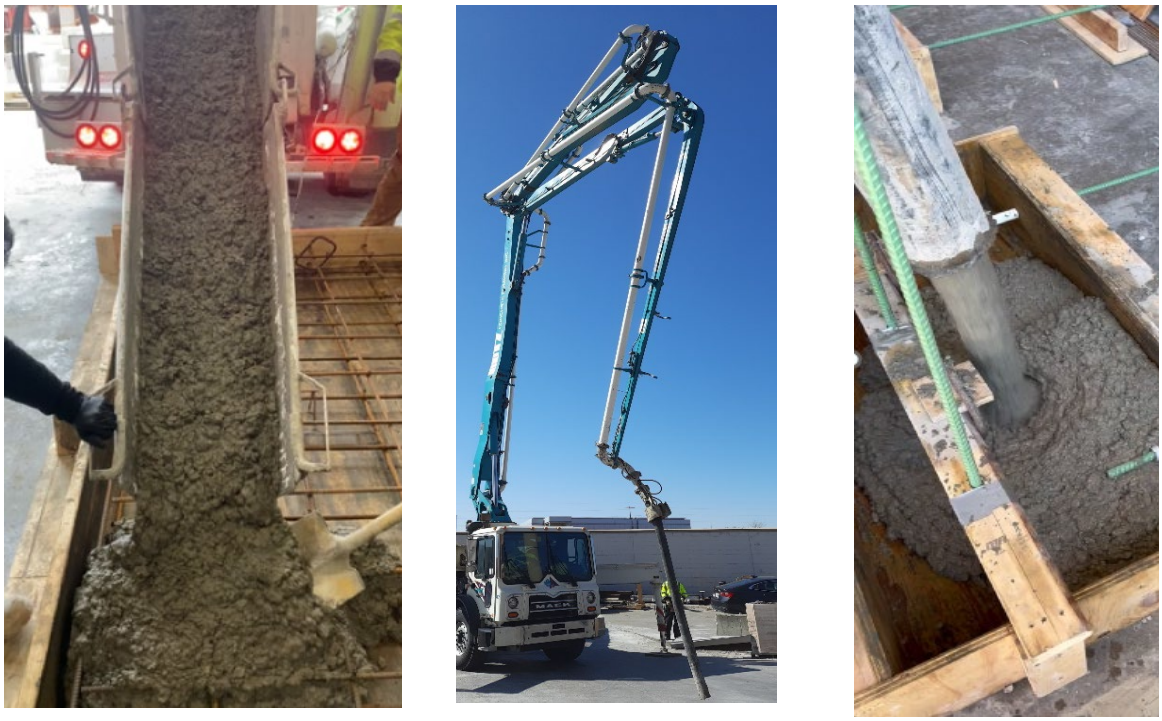

(a) (b) (c)

Figure 5.3 (a) Concrete placement using truck chute, (b) 100-ft long pump hose, and (c) concrete placement using concrete pump

Placement of RCMC mixes using either the truck chute or concrete pump was successful except when using the O47BD-R150 mixture as the concrete was too runny and some bleeding was observed during pumping as shown in Figure 5.4. Adjusting the dosage of the high-range water-reducing admixture or using viscosity modifying admixtures could address this problem. A mechanical vibrator was used for consolidation in all specimens.

Figure 5.4 Bleeding of O47BD-R150 mix while pouring

The specimens were then covered with plastic sheets as shown in Figure 5.5 and kept inside the lab at room temperature to cure for seven days. Cylinders were kept in their molds beside the specimens to regulate the curing conditions. Forms were stripped after seven days and the slabs were stacked in the lab until testing.

Figure 5.5 Curing of specimen in the mockup

5.5 Fresh Properties

Table 5.2 shows the slump and air content of all the mixtures directly upon arrival (i.e. initial) and after casting the specimen (i.e. final). The high slump of the O47BD-R100 and O47BR-R150 mixes is attributed to the high dosage of high-range water-reducing admixture needed for pumping. The air content was within the allowable range for all mixes except O47BR-R150, which demonstrated some bleeding as discussed earlier.

Table 5.19 Fresh properties of ready-mix concrete

Mix ID	Slump (in.)		Air Content (%)	
	Initial	Final	Initial	Final
47BD	3.00	2.00	-	-
O47BD-R50	4.50	4.25	6.75	6.25
O47BD-R100	6.75	6.50*	6.50	6.00*
O47BD-R150	7.50	6.75*	5.25	4.25*

* after pumping

5.6 Structural Performance

The compressive strength of all four mixes was determined at different ages using 4 in. x 8 in. cylinders. Figure 5.6 shows the average and standard deviation of three-cylinder compressive strength tests at 4, 7, 14, and 28 days. All the mixes achieved the NDOT-required 4000 psi compressive strength by 28 days. Although mixes with reduced cementitious materials content had slightly lower early strength, their 28-day strength was similar or sometimes better than the reference mix, which could be attributed to the optimized aggregate gradation that creates better aggregate interlock.

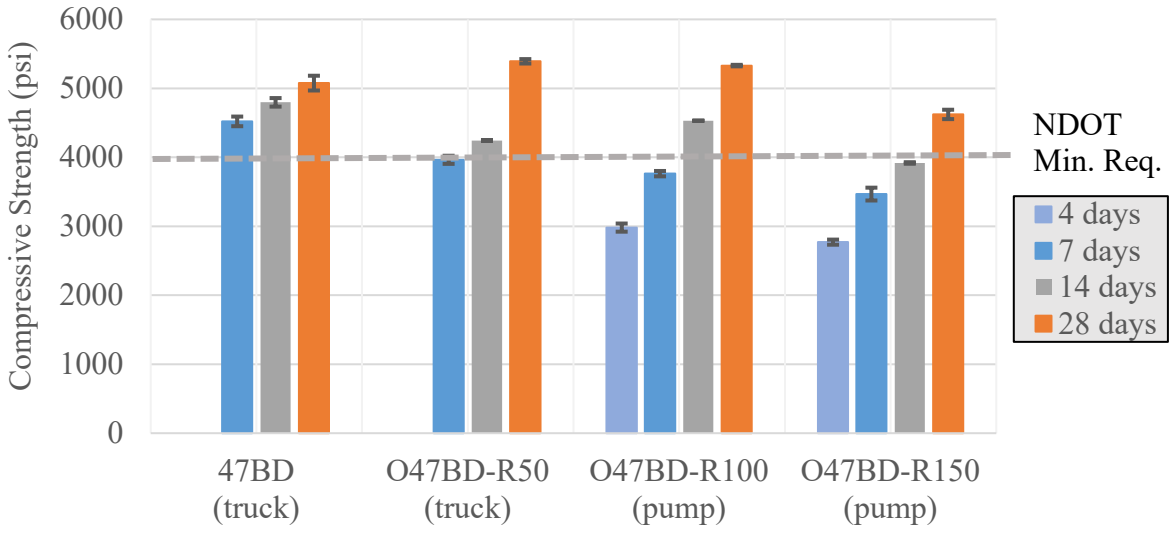

Figure 5.6 Cylinder compressive strength of concrete from ready-mix

A three-point bending test was conducted to evaluate the structural performance of the four slab specimens after achieving 4000 psi compressive strength. Figure 5.7 shows a schematic diagram of the test setup, while Figure 5.8 shows a photo of the test setup in the lab. The flexural capacity of each slab was calculated using the AASHTO LRFD strength design method for doubly reinforced concrete sections. Since the slab thickness slightly varies, design calculations for each slab are presented in Appendix A. Steel rollers were used to support the specimen, steel HSS beams with pads were used for loading, and steel spreader I-beams were used to distribute the ram load to the loading beams. The Bridge Diagnostics Inc. (BDI) system was used for instrumenting the specimens. Two string potentiometers were used to measure the deflection of the slab at mid-span on both sides. Four strain transducers were attached to measure the strain at mid-span during loading in the top and bottom fibers of the slab on both sides. The slabs were loaded until failure and the load-deflection plots of the slabs were recorded as shown in Figure 5.9.

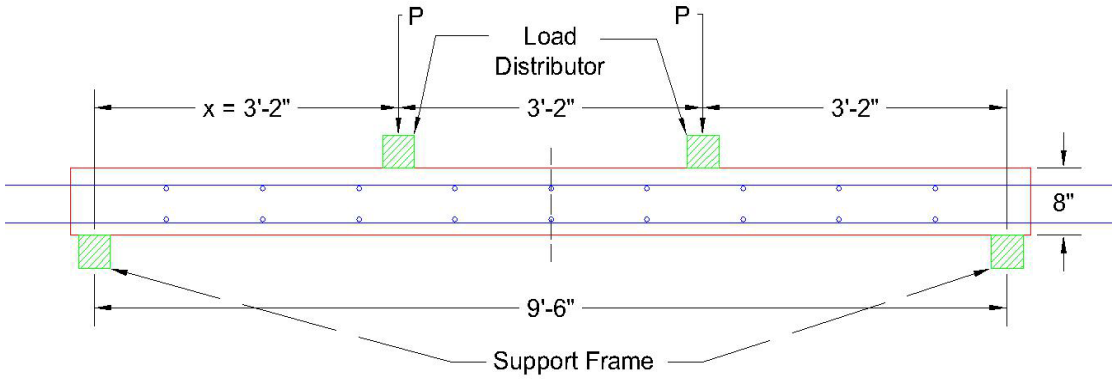

Figure 5.7 Schematic diagram of flexure test setup

Figure 5.8 Flexure test setup and instrumentation

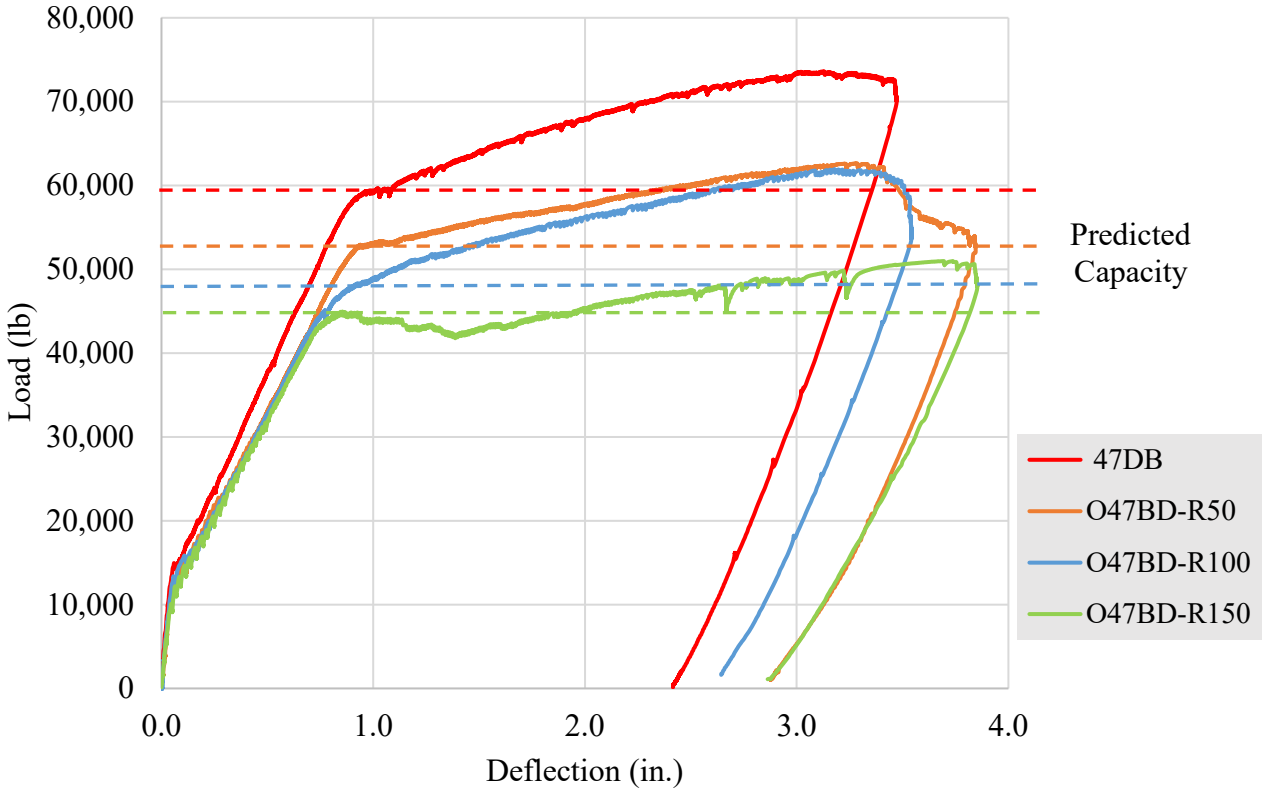

Figure 5.9 Load-deflection curves of the tested slabs

The load-strain curves are presented in Figure 5.10. Figure 5.11 shows the cracking and failure mode of each specimen. Figure 5.9 indicates that all the tested specimens exceeded their predicted capacity, but with different margins. While Figure 5.11 indicates that the 47BD, O47BD-R50, and O47BD-R100 specimens had similar behavior, specimen O47BD-R150 barely reached the predicted capacity and concrete spalling was observed at the time of testing. This indicates a weak concrete-rebar bond, which could be a result of the bleeding observed while pouring concrete.

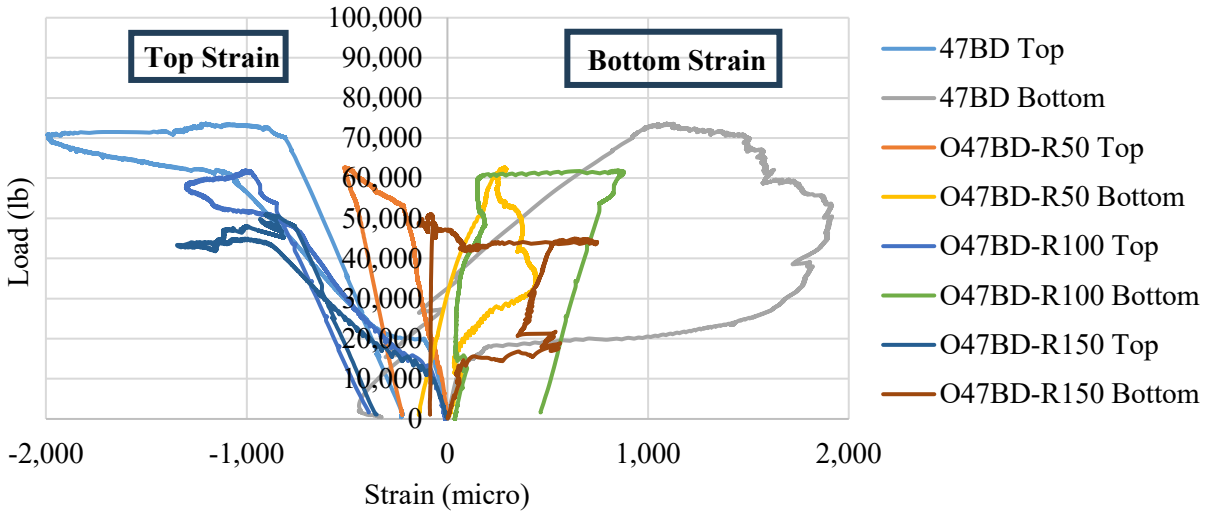

Figure 5.10 Load vs. strain curves of tested slabs

47BD

O47BD-R50

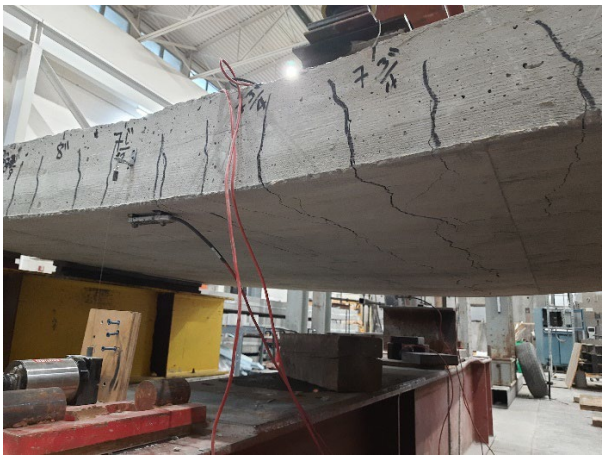

O47BD-R100

O47BD-R150

Figure 5.11 Slabs after flexure testing

Table 5.3 summarizes the predicted capacity, measured capacity, and their ratio for all specimens. The measured-to-predicted ratios for all specimens are higher than one, indicating satisfactory performance. However, the capacity of the specimen made using the O47BD-R150 mix was significantly lower than the others due to the bleeding observed during casting.

Table 5.20 Measured and predicted capacities of the tested slabs

Sample ID	Specimen Thickness (inch)	Predicted Capacity (kip)	Measured Capacity (kip)	Measured/Predicted Ratio
47BD	8.06	45.7	73.58	1.61
O47BD-R50	7.41	41.6	62.61	1.50
O47BD-R100	7.68	43.3	61.94	1.43
O47BD-R150	7.76	43.8	50.97	1.16

Concrete cores shown in Figure 5.12 were taken from each slab at each of the four corners after the flexure test. All the cores were ground, and three specimens were tested per slab at different ages ranging from 47 to 92 days. Figure 5.13 shows the test results indicating that all the mixes met the NDOT minimum required compressive strength except the O47BD-R150 mix. This low compressive strength could be the reason for the large cracks and spalling observed in the bending test of this slab.

Figure 5.12 Concrete cores taken from tested slabs

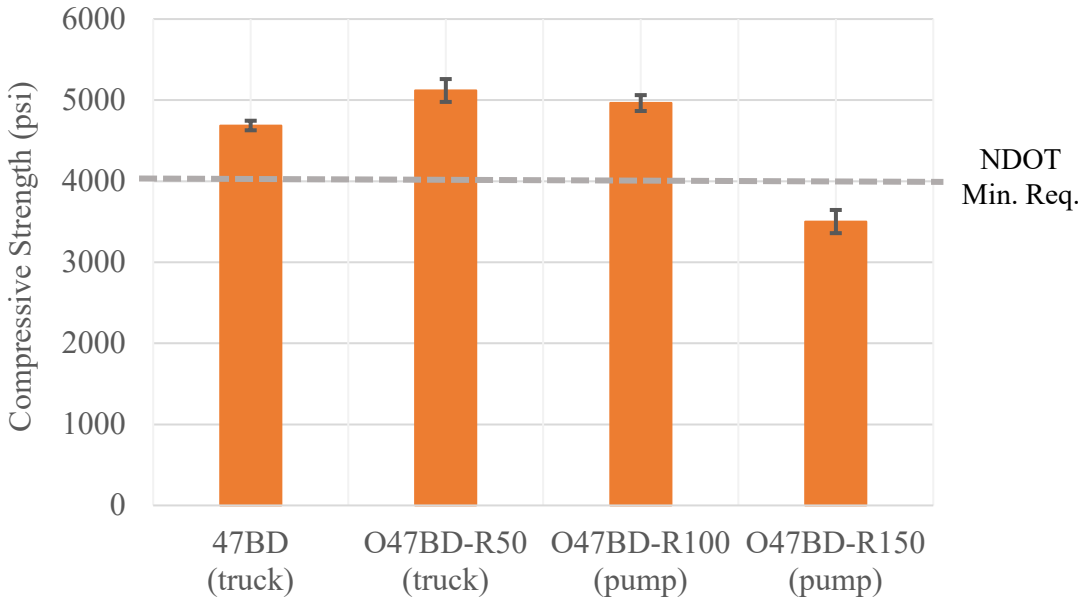

Figure 5.13 Concrete core compressive strength

5.7 Shear Strength of Concrete

Push-off specimens were cast monolithically without interface reinforcement from ready-mix concrete. Two samples were tested for every mix. The formwork of the specimen and the reinforcing details are presented in Chapter 3. The specimens were covered with plastic for seven days for curing and tested after the concrete compressive strength reached 4000 psi. A load cell and string potentiometer from the BDI system were used to measure the load and displacement during the shear test. The interface shear failure pattern is presented in Figure 5.14. AASHTO LRFD Bridge Design Specifications (2020) specifies the cohesion factor for the interface shear resistance of normal-weight concrete placed monolithically is 400 psi [section 5.8.4.3].

Figure 5.14 Shear failure (left) and failure plane of the specimens (right)

Figure 5.15 plots all the test results and indicates that all specimens meet the AASHTO LRFD predicted cohesion factor value regardless of the cementitious material content. This

could be attributed to the fact that cohesion is dependent on the aggregate interlocking system, which is improved in the optimized mixes. The shear interface of the specimens presented in Figure 5.14 after failure shows more aggregate in the RCMC mixes interface. Test results are also presented in Table 5.4. All the specimens failed in the shear test except sample-2 of the O47BD-R100 mix, which failed in the flexure test due to incorrect placement of the specimen reinforcement.

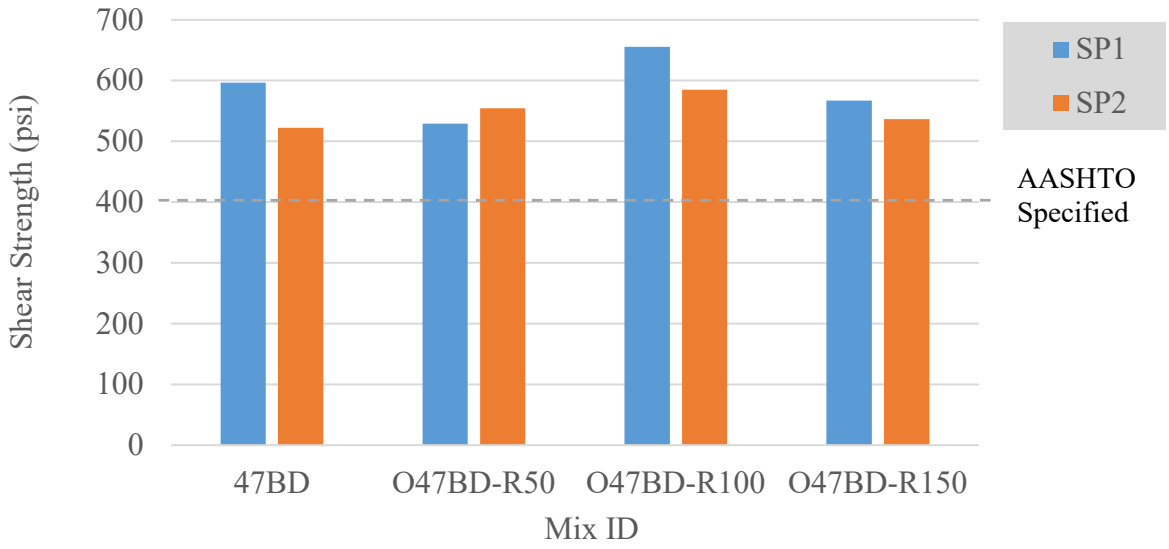

Figure 5.15 Shear strength comparison of mixes

Table 5.21 Shear strength of concrete

Mix ID	Specimen ID	Max. Load (lb)	Interface width (in.)	Stress (psi)
47BD	1	33,626	5.13	596
	2	28,489	4.96	522
O47BD-R50	1	30,077	5.17	529
	2	30,748	5.04	554
O47BD-R100	1	36,650	5.08	655
	2*	32,183	5.00	585
O47BD-R150	1	30,926	4.96	567
	2	30,231	5.13	536

* Not a shear failure

5.8 Concrete-Rebar Bond Strength

Two 4 ft x 2 ft x 0.67 ft specimens were cast per mix to perform three horizontal and three vertical concrete-rebar bond tests for every mix. The formwork and the sample after casting are presented in Figure 5.16 (a) and (b), respectively. The samples were covered with plastic for seven days for curing and tested after the concrete compressive strength reached 4000 psi. The specimens were tested with a BDI system load cell to measure the maximum load. Similar set-ups were used for horizontal and vertical bars as shown in Figure 5.16 (c) and (d), respectively.

(a)

(b)

(c)

(d)

Figure 5.16 (a) Formwork for bond samples, (b) Specimen after demolding, (c) Test setup for horizontal bars, and (d) Test setup for vertical bars

The concrete-rebar bond strength test results are presented in Table 5.5 and a summary is presented in Figure 5.17 using a bar chart. These strengths significantly exceed the one assumed for the design in section 5.11.2.1.1 of AASHTO LRFD Bridge Design Specification (2020) of Tension Development Length. The plot shows a reduction in the bond strength with the reduction of cementitious material content. However, all results are still much higher than calculated, which is approximately 0.5 ksi. The lowest bond strength was observed in the

O47BD-R150 mix, which explains the spalling of concrete cover observed in the bending test of the O47BD-R150 slab specimen.

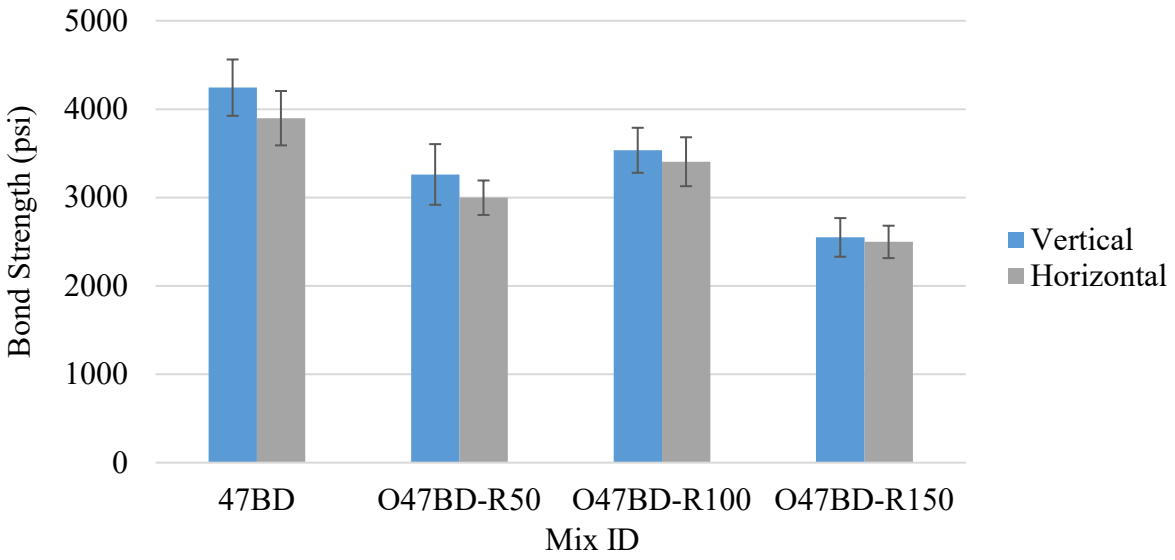

Figure 5.17 Concrete-rebar bond strength

Table 5.22 Concrete-rebar bond strength

Mix ID	Sample Orientation	Force (lb)	Bond Length (in)	Bond Area (sq.in.)	Bond Strength (psi)	Average Strength (psi)	SD	COV*
47BD	Vertical	27,794	3.125	6.14	4,530	4,243	319	7.5%
		26,142	3.250	6.38	4,097			
		25,735	3.125	6.14	4,194			
		25,748	3.125	6.14	4,196			
		24,093	3.250	6.38	3,776			
		27,498	3.000	5.89	4,668			
	Horizontal	16,250	2.375	4.66	3,485	3,898	308	7.9%
		16,056	2.250	4.42	3,634			
		22,680	3.000	5.89	3,850			
		26,511	3.250	6.38	4,154			
		23,351	3.000	5.89	3,964			
		27,430	3.250	6.38	4,298			

Mix ID	Sample Orientation	Force (lb)	Bond Length (in)	Bond Area (sq.in.)	Bond Strength (psi)	Average Strength (psi)	SD	COV*
O47BD-R50	Vertical	25,390	3.375	6.63	3,831	3,261	343	10.5%
		18,910	3.125	6.14	3,082			
		21,617	3.250	6.38	3,388			
		18,690	3.250	6.38	2,929			
		18,148	3.125	6.14	2,958			
		19,900	3.000	5.89	3,378			
	Horizontal	20,820	3.250	6.38	3,263	2,998	195	6.5%
		20,968	3.500	6.87	3,051			
		18,114	3.375	6.63	2,733			
		19,200	3.125	6.14	3,129			
		18,025	3.250	6.38	2,825			
		18,320	3.125	6.14	2,986			
O47BD-R100	Vertical	16,081	3.125	6.14	2,621	3,534	255	7.2%
		16,138	3.125	6.14	2,630			
		22,994	3.125	6.14	3,747			
		21,800	3.000	5.89	3,701			
		18,773	3.000	5.89	3,187			
		20,632	3.000	5.89	3,503			
	Horizontal	24,067	3.250	6.38	3,771	3,405	277	8.1%
		20,570	3.000	5.89	3,492			
		21,510	3.125	6.14	3,506			
		16,774	2.750	5.40	3,107			
		19,324	3.125	6.14	3,149			
		23,771	2.875	5.65	4,211			
O47BD-R150	Vertical	15,336	3.125	6.14	2,499	2,549	219	8.6%
		15,693	3.125	6.14	2,558			
		16,786	3.250	6.38	2,630			
		17,587	3.125	6.14	2,866			
		16,121	3.750	7.36	2,189			
		17,515	3.500	6.87	2,549			
	Horizontal	12,577	3.500	6.87	1,830	2,498	183	7.3%
		16,556	3.500	6.87	2,409			
		17,456	3.500	6.87	2,540			
		13,160	3.000	5.89	2,234			
		19,972	3.750	7.36	2,712			
		17,823	3.500	6.87	2,593			

* Coefficient of Variation (COV)

5.9 Restrained Shrinkage

Restrained shrinkage specimens were taken from the ready-mix concrete to confirm the test results obtained earlier using lab-mix concrete for all mixes. The results presented in Figure 5.18 show a similar trend as observed in the lab mixes except for O47BD-R150. The bleeding observed after placing the O47BD-R150 mix resulted in lower compressive strength and earlier cracking than expected.

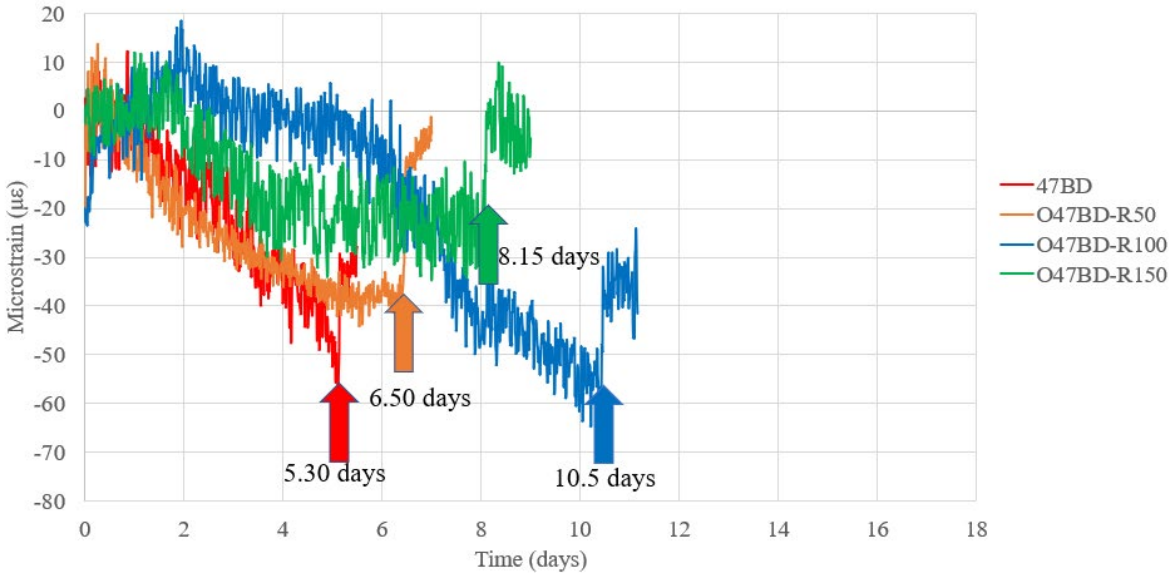

Figure 5.18 Cracking time in restrained shrinkage test

5.10 Summary of Production Mockup

Production and testing of mockup specimens demonstrated that the O47BD-R50 and O47BD-R100 mixes have very similar behaviors in flexure, bond, and shear tests compared to the reference mix. Lower compressive strength, shear strength, and a shorter cracking time were observed for the O47BD-R150 mix, indicating the necessity for adjustment of admixtures to ensure the stability of the mix. No issues were found with pumpability of the new mixes.

Chapter 6 Conclusions and Recommendations

6.1 Conclusions

The main goal of this study is to develop and evaluate the performance of reduced cementitious materials content concrete mixtures for bridge decks and rails. The study demonstrated that using optimized aggregate gradation, it is possible to reduce the cementitious material content in bridge decks and rails by up to 23% without significantly compromising their performance. Based on the results of this experimental study, the following conclusions are drawn:

1. Reduced cementitious materials concrete (RCMC) mixtures have less free shrinkage than that of the conventional 47BD mixture. This reduction of free shrinkage is proportionate to the amount of cementitious materials reduction, which is in agreement with the literature.
2. RCMC mixtures take longer to crack and have a lower shrinkage rate in the restrained shrinkage test than the conventional 47BD mixture. This allows concrete to gain strength and resistance to cracking given the same curing conditions and period.
3. RCMC mixtures have slightly lower workability in the slump and vibrating L-box tests than the conventional 47BD mixture, which requires a slightly higher dosage of superplasticizer to achieve the desired workability.
4. Pumping RCMC mixtures with up to 100-lbs reduction in the cementitious material content is satisfactory. For the RCMC mixture with 150-lbs reduction in the cementitious material content, extra attention should be given to mixture workability and stability to avoid aggregate segregation.
5. RCMC mixtures with 100-lbs and 150-lbs reduction in the cementitious material content have significantly longer initial and final set times than the conventional 47BD and

RCMC mixtures with 50 lbs reduction. This could be attributed to the higher dosage of superplasticizers used.

6. There is no significant change in the 28-day compressive strength of RCMC mixtures compared to the conventional 47BD mixture. However, a slightly slower strength gain was observed in the RCMC mixtures at an early age.
7. Most mechanical properties, such as modulus of rupture, modulus of elasticity, concrete-to-concrete bond strength (i.e., slant shear strength), and shear strength, are not significantly affected by the reduction of the cementitious material content in the RCMC mixtures.
8. RCMC mixtures with 50-lbs and 100-lbs reduction in the cementitious material content have comparable flexural strengths and bond strengths with reinforcing steel to those of the conventional 47BD, which was not the case of RCMC mixture with 150-lb reduction as it demonstrated slightly lower flexural and bond strength.
9. RCMC mixtures demonstrated comparable or even better durability than that of the conventional 47BD mixture with respect to freeze-and-thaw resistance, surface/bulk resistivity, and rapid chloride penetration tests.

6.2 Recommendations for Future Work

Given the scope of this study and its findings, below are areas recommended for future research:

1. Conduct a field-scale demonstration using the RCMC mixtures in the construction of bridge decks and rails to monitor their performance for an extended period of time using visual inspection and appropriate instrumentation to accurately assess the reduction in shrinkage cracking in a real environment.

2. Evaluate the possibility of reducing the moist curing period when RCMC mixtures are used to allow traffic on the bridge earlier and reduce the user cost.
3. Make necessary adjustments to the RCMC mixture with 150-lbs reduction of the cementitious material content to ensure successful pumpability for bridge deck construction.
4. Evaluate the impact of the longer set times for RCMC mixtures on the construction practice and cost with potential measures to reduce setting time, especially during time-sensitive bridge projects.

References

Abdigaliyev, A., Kim, Y., and Hu. J. (2020). *Application of Internal Curing to Improve Concrete Bridge Deck Performance.* Nebraska Department of Transportation, Report No. SPR-P1(19) M083. https://dot.nebraska.gov/media/113555/ndot-m083-internal-curing-project-report_final.pdf

Almusallam, A. A., Maslehuddin, M., Abdul-Waris, M., & Khan, M. M. (1998). Effect of mix proportions on plastic shrinkage cracking of concrete in hot environments. *Construction and Building Materials,* 12(6-7), 353-358.

American Association of State Highway and Transportation Officials (2020). *AASHTO LRFD Bridge Design Specifications*, 9th Ed., customary U.S. units. American Association of State Highway and Transportation Officials.

Ardeshirilajimi et al. (2016). *Bridge decks: Mitigation of cracking and increased durability*. University of Illinois at Urbana-Champaign and Saint Louis University. https://apps.ict.illinois.edu/projects/getfile.asp?id=4980

Bridge Office Policies and Procedures, BOPP (2016). Nebraska Department of Transportation (NDOT), NE.

California Department of Transportation (Caltrans), 2015. *Standard Specifications*. State of California, California State Transportation Agency, Department of Transportation. Sacramento, CA. http://ppmoe.dot.ca.gov/hq/esc/oe/construction_contract_standards/std_specs/2015_StdSpecs/2015_StdSpecs.pdf

CEB-fib. 2000. "Bond of Reinforcement in Concrete." *fib*, Bulletin No. 10, Lausanne, Switzerland, 427.

Chaunsali, P., Lim, S., Mondal, P., & Foutch, D. (2013). *Bridge decks: Mitigation of cracking and increased durability*. University of Illinois at Urbana-Champaign. https://apps.ict.illinois.edu/projects/getfile.asp?id=3099

Construction and Material Specification, (2019). Ohio Department of Transportation (ODOT), OH. https://www.dot.state.oh.us/Divisions/ConstructionMgt/OnlineDocs/Specifications/2019CMS/2019_CMS_12122018_for_web_letter_size.pdf

Dam, T.V., Duffala, N., and Stempihar, J. (2016). *Phase I: Minimization of Cracking in New Concrete Bridge Decks.* Nevada Department of Transportation, Report No. 530-14-803. https://www.dot.nv.gov/home/showdocument?id=9373

Development of Specifications for High-Performance Fiber Concrete for Nevada. Report No. 366-16-803 (July 2020.). Nevada Department of Transportation. https://www.dot.nv.gov/home/showpublisheddocument/18974/637509735528100000

Development of Specifications for High-Performance Fiber Concrete for Nevada. Report No. 366-16-803 (July 2020.). Nevada Department of Transportation. https://www.dot.nv.gov/home/showpublisheddocument/18974/637509735528100000

Hu, J., & Wang, K. (2005, August). Effects of aggregate on flow properties of mortar. In *Proceeding of the Mid-Continent Transportation Research Symposium* (p. 8).

Khajehdehi, R., Darwin, D., & Feng, M. (2021). Dominant Role of Cement Paste Content on Bridge Deck Cracking. *Journal of Bridge Engineering*, *26*(7), 04021037.

Khajehdehi, Rouzbeh & Darwin, David. (2018). Controlling Cracks in Bridge Decks. *Structural Engineering and Engineering Materials*, SM Report No. 129. DOI: 10.13140/RG.2.2.33376.33288.

Khan, M., and Ali, M. (2016). *Use of glass and nylon fibers in concrete for controlling early age micro cracking in bridge decks*. Construction and Building Materials, 125 (2016) 800–808.

Lindquist, W., Darwin, D., and Browning, J. (2008). *Development and construction of Low-Cracking High-Performance Concrete (LC-HPC) Bridge decks: Free shrinkage, mixture optimization, and Concrete production.* The University of Kansas Center for Research, Inc. SM Report No. 92. https://kuscholarworks.ku.edu/handle/1808/19944

Mamirov, M. Hu, J, and Kim, Y. (2021). *Effective Reduction of Cement Content in Pavement Concrete Mixtures Based on Theoretical and Experimental Particle Packing Methods*. Journal of Materials in Civil Engineering, V 33, Issue 10, Pages 04021277

Mattock, A. H., and Hawkins, N. M. 1972. "Shear Transfer in Reinforced Concrete." *PCI Journal*, Vol. 17, No. 2, 55–75.

Missouri Standard Specifications for Highway Construction, (2019). Missouri Department of Transportation (MoDOT), MO. https://www.modot.org/sites/default/files/documents/2019_MO_Std_Spec_Gen_Supp_%28July%202019%29_1.pdf

National Bridge Inventory – Based on the Coding Guide (2022). U.S. Department of Transportation website, www.fhwa.dot.gov/bridge/nbi.cfm

Deng, Y., Phares, B., and Harrington, D. (2016). Causes of Early Cracking in Concrete Bridge Decks. *Moving Advancement into Practice*, Iowa State University.

Qiao, P., McLean, D. I., & Zhuang, J. (2010). *Mitigation strategies for early-age shrinkage cracking in bridge decks.* Department of Civil & Environmental Engineering, Washington State University. https://www.wsdot.wa.gov/research/reports/fullreports/747.1.pdf.

RILEM/CEB/FIP. 1970. "Test and Specifications of Reinforcement for Reinforced and Pre-Stressed Concrete: Four Recommendations of the RILEM/CEB/FIP, 2: Pullout Test." *Materials and Structures*, Vol. 3, No. 15, 175–178.

Self-Consolidating Concrete for Cast-in-Place Bridge Components. Report 819 (2016). National Cooperative Highway Research Program. DOI 10.17226/23626

Smith, M. R. and Collis, L. 2001. *Aggregates – Sand, Gravel and Crushed Rock Aggregates for Construction Purposes* (3rd edition). The Geological Society London, Chapter 8, pp.199-224.

Standard Specification for Highway Construction (2017). *Nebraska Department of Transportation* (NDOT), NE.

Standard Specifications for Construction, (2020). Michigan Department of Transportation (MDOT), MI. https://www.michigan.gov/documents/mdot/MDOT_2020_Spec_Book_DRAFT_July_2020_697214_7.pdf

Standard Specifications for Construction, Volume 1 and Volume 2 (2020). Minnesota Department of Transportation (MnDOT), MN. http://www.dot.state.mn.us/pre-letting/spec/

Standard Specifications for Highway and Bridge Construction, (2015). Iowa Department of Transportation (IOWADOT), IOWA. https://www.iowadot.gov/specifications/pdf/completebook.pdf

Standard Specifications for Highway and Structure Construction, (2022). Wisconsin Department of Transportation, WI. https://wisconsindot.gov/rdwy/stndspec/ss-00-10.pdf

Standard Specifications for Highway Construction, (2017). Nebraska Department of Transportation (NDOT), NE. https://dot.nebraska.gov/media/10343/2017-specbook.pdf

Standard Specifications for Road and Bridge Construction, (2014). Nevada Department of Transportation (NEVADADOT), NV. https://www.dot.nv.gov/home/showdocument?id=6916

Standard Specifications for Road and Bridge Construction, (2016). Illinois Department of Transportation (IDOT), Illinois. https://idot.illinois.gov/Assets/uploads/files/Doing-Business/Manuals-Guides-&-Handbooks/Highways/Construction/Standard-Specifications/Standard%20Specifications%20for%20Road%20and%20Bridge%20Construction%202016.pdf

Standard Specifications for Road and Bridge Construction, (2019). Colorado Department of Transportation (CDOT), CO. https://www.codot.gov/business/designsupport/cdot-construction-specifications/2019-construction-specifications/2019-specs-book/2019-standard-specifications

Standard Specifications for Road and Bridge Construction, (2020). North Dakota Department of Transportation (NDDOT), ND. https://www.dot.nd.gov/divisions/environmental/docs/supspecs/2020%20Standard%20Specifications%20for%20Road%20and%20Bridge%20Construction.pdf

Standard Specifications for Road and Bridge Construction, (2021). Wyoming Department of Transportation (WYDOT), WY. https://www.dot.state.wy.us/files/live/sites/wydot/files/shared/Construction/2021%20Standard%20Specifications/Wyoming%202021%20Standard%20Specifications%20for%20Road%20and%20Bridge%20Construction.pdf

Standard Specifications for Roads and Bridges, (2015). South Dakota Department of Transportation (SDDOT), NE. https://dot.sd.gov/media/documents/2015_SDDOT_SpecBook.pdf

Standard Specifications for State Road & Bridge Construction, (2015). Kansas Department of Transportation (KDOT), KS. https://www.ksdot.org/burconsmain/specprov/2015specprov.asp

Standard Specifications, (2020). Indiana Department of Transportation (INDOT), IN. https://www.in.gov/dot/div/contracts/standards/book/sep19/2020%20INDOT%20Standard%20Specifications.pdf

Wan, B., Foley, C., & Komp, J. (2010). *Concrete cracking in new bridge decks and overlays*. Department of Transportation, Marquette University. https://epublications.marquette.edu/cgi/viewcontent.cgi?article=1010&context=transportation_widot

Xi, Y., Shing, B., & Xie, Z. (2001). *Development of optimal concrete mix designs for Bridge Decks*. Department of Civil, Environmental and Architectural Engineering of University of Colorado, Boulder. https://www.codot.gov/programs/research/pdfs/2001/bridgedeckmix.pdf

Xi, Y., Shing, B., and Xie, Z. (2001). Development of Optimal Concrete Mix Designs for Bridge Decks. *The Colorado Department of Transportation*, Report No. CDOT-DTD-R-2001-11.

Appendices

Appendix A – Flexural Strength Calculations of Tested Slabs

Appendix B – Shop Tickets of Ready Mix Concrete